STOCHASTIC MODELING-BASED DGPS ESTIMATION ALGORITHM

THESIS

James T. Broaddus, Captain, USAF

AFIT/GE/ENG/00M-06

DEPARTMENT OF THE AIR FORCE
AIR UNIVERSITY

AIR FORCE INSTITUTE OF TECHNOLOGY

Wright-Patterson Air Force Base, Ohio

20000815 171

The view expressed in this thesis are those of the author and do not reflect the official

policy or position of the Department of Defense or the U. S. Government.

STOCHASTIC MODELING-BASED DGPS ESTIMATION ALGORITHM

THESIS

Presented to the Faculty of the Graduate School of Engineering and Management

of the Air Force Institute of Technology

In Partial Fulfillment of the

Requirements for the Degree of

Master of Science in Electrical Engineering

Todd Broaddus, B.S.E.E.

Captain, United States Air Force

March, 2000

STOCHASTIC MODELING-BASED DGPS ESTIMATION ALGORITHM

Todd Broaddus, B.S.E.E.
Captain, United States Air Force

Approved:

M. Pachter   _3 March 2000_
Dr. Meir Pachter   Date
Professor, Thesis Advisor

M. M. Miller   _3 Mar 00_
Mikel M. Miller, PhD, Lt Col, USAF   Date
Assistant Professor, Thesis Reader

John F. Raquet   _3 MAR 00_
John F. Raquet, PhD, Capt, USAF   Date
Assistant Professor, Thesis Reader

Preface

I would like to thank my committee members for their time, patience and understanding during the development of this thesis.

Table of Contents

List of Figures

List of Tables

Abstract

A Kinematic Differential Global Positioning System (KDGPS) algorithm is

developed. A number of mobile receivers is considered, one of which will be designated

the 'reference station' which will have known position and velocity information at the

beginning of the time interval examined. Satellite clock biases are used to model

Selective Availability. The measurement situation on hand is properly modeled and a

centralized estimation algorithm processing several epochs of data. The effect of

uncertainty in the reference receiver's position and the level of receiver noise is

examined. Monte Carlo simulations are performed to examine the ability of the

algorithm to correctly estimate the non-reference mobile users' position and velocity

despite substantial satellite clock errors and receiver measurement noise.

Nomenclature

N	Number of GPS pseudorange measurements available (T / ΔT)
n	Number of satellites visible
ΔT	Sampling interval
T	Temporal horizon (time duration of interest)
(x_j, y_j, z_j)	User position at discrete time 'j'
$x_{s_{i,j}}$	i^{th} Satellite position at time j
$\rho_{i,j}$	Distance from the user's receiver to satellite i at time j
Z_i	i^{th} GPS pseudorange measurement
τ	User's receiver range equivalent clock bias
$\dot{\tau}$	User's receiver range equivalent clock drift
i	Satellite number, 1, 2, ..., n
j	Discrete time instance, 0, 2, ...N
k	Number of users, 1, 2, ..., m
m	Number of reference stations
$\hat{x}$	Position estimate
θ	Parameter vector of interest (positions, velocities, clock biases)

Batch Processing of GPS Signals

1 Introduction

A kinematic DGPS algorithm is developed to handle GPS pseudorange measurements from multiple receivers obtained during multiple measurement epochs and process the data in batch form. The proposed algorithm is tested to estimate position and velocity information of two simulated, mobile users.

1.1 Background

There are a growing number of applications requiring the ability to obtain real-time, kinematic positioning of high altitude formation-flying vehicles. These include Low Earth Orbit (LEO) military satellite formations for earth observation/surveillance, and NASA's proposed New Millennium program [5]. Therefore, formations of satellites might replace large, complex, satellites and allow lower overall cost and a higher degree of redundancy [8]. Research is being conducted to replace or augment the existing inertial navigation systems on board satellites with GPS receivers to allow meeting the stringent positioning requirements for the formation.

While the majority of current research is focused on utilizing carrier phase GPS techniques to acquire position and velocity information for each epoch [1, 2, 4, 8, 11], this study will examine the general principals and trends in utilizing pseudorange measurements only over a series of measurement epochs.

1.2 Problem Statement

The integration of kinematic modeling and centralized, or batch, processing of the GPS information is examined for two mobile users. In order to obtain accurate positioning and velocity information, Differential GPS (DGPS) techniques will be utilized. Generally, conventional DGPS techniques remove common errors by directly differencing a derived error term from the mobile user's pseudorange. The developed algorithm will attempt to remove these errors by implicit differencing incurred during batch processing. In addition, the effect of uncertainty in the reference receiver's position and the amount of receiver noise is investigated to determine how this will influence the algorithm's ability to derive the desired information.

1.3 Summary of Current Knowledge

Investigation into the absolute and relative positioning of vehicles by use of GPS signals is well documented [6, 9]. These include stand-alone and DGPS techniques utilizing either pseudorange measurements or carrier phase measurements. These techniques are briefly described in Chapter 2.

Using GPS for relative and absolute positioning of formation flying vehicles is relatively new [1, 2, 4, 8]. The majority of the current research involves utilizing the Carrier Phase DGPS techniques for tracking and controlling vehicles. Simulated results indicate that $\leq$ 2cm rms position errors are possible [1].

1.4 Scope

The centralized algorithm developed to derive the user's position and velocity will be simulated using several different sets of parameters. These parameters include varying degrees of certainty in the reference receiver's position and velocity as well as different levels of receiver noise. Results from these simulations will be analyzed to determine the algorithms ability to handle both GPS measurements and derive the user's position and velocity.

1.5 Assumptions

Typical of any simulation which attempts to examine a concept, assumptions were made in this thesis to facilitate development of the models and implementation of the developed algorithm. These assumptions are:

a) Ephemeris errors associated with each satellite are not modeled. This will leave GPS satellite clock errors as the only error term induced on the GPS signal by the GPS satellite constellation.

b) The number of satellites in view is held constant during the simulation.

c) The two mobile users simulated are moving parallel to each other at an altitude of approximately 180 nautical miles above the surface of the earth.

d) The effects of ionospheric disturbances will not be modeled.

1.6   Overview of Thesis

Chapter 2 presents the background theory used to develop the GPS position and velocity determination mathematical models. The theory summarized in this chapter was used as the basis to develop the theory behind the centralized batch-processing algorithm.

Chapter 3 describes the theory and the implementation methodology for the developed centralized batch-processing algorithm.

Chapter 4 presents the results of each scenario simulated in this study. An analysis and interpretation of the results is also presented in this chapter.

Chapter 5 summarizes the research effort and provides recommendations for future enhancements and research areas as an extension to this work.

2 Theory

2.1 Overview

This chapter describes the theory behind the development of the batch-processing algorithm tested in the Monte Carlo simulations. In addition, the stand-alone and DGPS algorithms used to develop the algorithm used in this research are briefly described.

2.2 Global Positioning System

The Global Positioning System consists of a constellation of 24 satellite vehicles (SV) in six orbital planes inclined at 55 degrees at an altitude of 20,200km. The constellation continually broadcasts signals that can be utilized by a receiver on the user's platform. The GPS receiver determines the range from each visible satellite to the user's platform. This measured range is called a "pseudorange" since there are errors present on the GPS signal.

Since there are four unknown parameters involved with GPS positioning (3 Cartesian position parameters x, y, and z, and GPS time) at least four GPS SVs within view of the receiver are required for a solution. The pseudoranges from the SVs are used to determine the user's position with respect to Earth. Figure 1 shows a typical GPS scenario. SV geometry plays an important part in GPS positioning. Poor SV geometry with respect to the receiver produces high Geometric Dilution Of Precision (GDOP), which can wreak havoc on GPS position solutions [6].

Civil Standard Positioning Service (SPS) receivers are subjected to Selective

Availability (SA), an additional error intentionally injected onto the GPS signal by the

GPS Mission Control Segment. SA decreases the positioning accuracy of stand-alone

receivers to within 100-meters RMS. Military receivers utilize de-encryption techniques

to remove SA and provide position accuracy of 10-meters root-mean-square (RMS) [6].
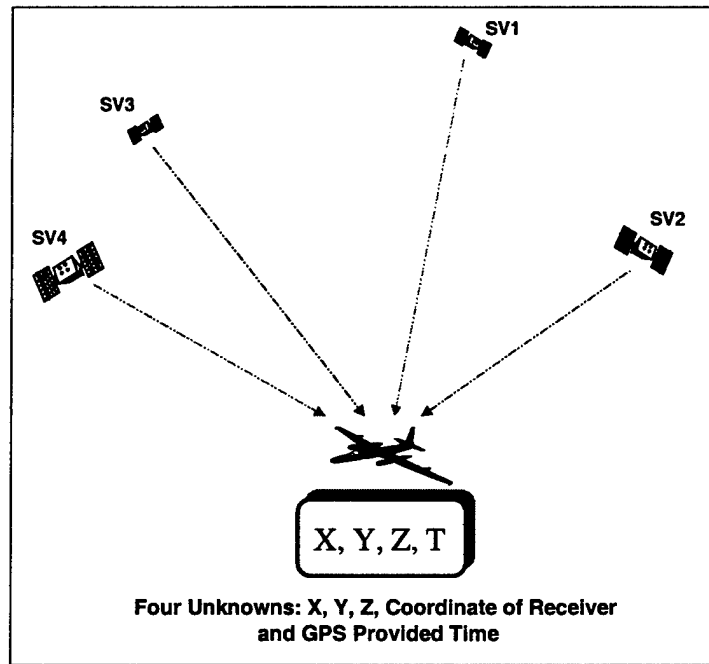
Figure 1.   GPS Scenario [12]

2.2.1 *Stand-Alone GPS Positioning*

Single point, or stand alone, GPS techniques utilize signals broadcast from the GPS

satellites as depicted in Figure 1. First, a nominal state (consisting of user position

coordinates and receiver clock error) can be represented as

$$\hat{\mathbf{x}}_u = \begin{bmatrix} \hat{x} \\ \hat{y} \\ \hat{z} \\ c\hat{\delta t} \end{bmatrix} = approximate\ state \qquad (2\text{-}1)$$

At a given measurement epoch, the GPS receiver generates a set of n pseudorange equations (where n is the number of satellites visible to the receiver). The pseudorange from the user receiver to the ith satellite is the sum of the true range plus the receiver range equivalent clock error (i.e., after ionospheric, tropospheric, etc. errors have been removed)

$$\rho_{user}^i = \sqrt{(x_i - x_{user})^2 + (y_i - y_{user})^2 + (z_i - z_{user})^2} + c\delta t \qquad (2\text{-}2)$$

where

$(x_{user}, y_{user}, z_{user})$	= ECEF position coordinates of the user (m)
(x_i, y_i, z_i)	= ECEF position coordinates of the ith satellite (m)
$c\delta t$	= Range equivalent receiver clock error (m)

Although these equations are generally non-linear, several solution techniques have been developed. These include closed form solutions, Kalman filtering and Iterated Least Square (ILS) techniques based on linearization [6, 9]. Since the ILS algorithm is most commonly used, it will be subsequently explained.

Since the position of the user is not known, an estimate of the user position $(\hat{x}, \hat{y}, \hat{z})$ is used to generate a set of estimated pseudoranges to each of the n satellites, i.e.

$$\hat{\rho}_n^i = \sqrt{(x_i - \hat{x}_{user})^2 + (y_i - \hat{y}_{user})^2 + (z_i - \hat{z}_{user})^2} + c\delta t \qquad (2\text{-}3)$$

The relationship between the true and the estimated position with errors can be written as

$$\mathbf{x}_u = \hat{\mathbf{x}}_u + \Delta\mathbf{x}_u \qquad (2\text{-}4)$$

The approximated pseudorange equations (Equation (2-3)) are then linearized using a first order Taylor series approximation to yield

$$\Delta\boldsymbol{\rho} = \mathbf{H}\Delta\mathbf{x} - c\delta t_u \qquad (2\text{-}5)$$

where

$$\Delta\rho = \begin{bmatrix} \Delta\rho_1 \\ : \\ \Delta\rho_n \end{bmatrix} \quad H = \begin{bmatrix} a_{x1} & a_{y1} & a_{z1} & 1 \\ : & : & : & : \\ a_{x1} & a_{y1} & a_{z1} & 1 \end{bmatrix} \quad \Delta x = \begin{bmatrix} \Delta x_u \\ : \\ -c\Delta\delta t \end{bmatrix} \qquad (2\text{-}6)$$

The values (a_{x1}, a_{y1}, a_{z1}) are unit vectors from the linearization point to the ith satellite.

Solving equation (2-5) has the solution

$$\Delta x = H^{-1}\Delta\rho \qquad (2\text{-}7)$$

The values obtained for Δx are used to update equation (2-4) for the users position.

There are three possible cases to be considered. If there are fewer than four satellite

pseudoranges available, the position cannot be determined since Δx cannot be resolved.

If there are exactly 4 pseudoranges, there will be a unique solution. However, if there are

more than four satellites visible, as is generally the situation, an overdetermined linear

system is obtained, and no solution will be available that will perfectly solve the equation

in Δx. For this case, the least squares solution concept can be utilized.

Basic least squares techniques yield the solution

$$\Delta x = (H^T H)^{-1} H^T \Delta\rho \qquad (2\text{-}8)$$

Alternatively, a weighted least squares solution

$$\Delta x = (H^T C_\rho^{-1} H)^{-1} H^T C_p^{-1} \Delta\rho \qquad (2\text{-}9)$$

can be used when it is believed (as is usually the case) that the pseudorange

measurements have different error statistics or that the pseudorange measurement errors

are correlated. C_ρ is the measurement error covariance matrix. (Diagonal terms are

measurement error variances and off-diagonal terms show cross-correlation between measurement errors).

For the over-determined case, there is generally no solution for Δx that exactly solves the measurement equation. However, measurement residuals, v, can be applied to the measurements which would result in

$$\Delta\rho = H\Delta x + v \tag{2-10}$$

or

$$v = \Delta\rho - H\Delta x \tag{2-11}$$

Single point positioning estimates only receiver clock errors, and requires a correction for the satellite clock error. Satellite clock error corrections can be accomplished as described in ICD-GPS-200C

$$\rho_{corrected} = \rho + c\Delta t_{sv} \tag{2-12}$$

where,

Δt_{sv}	$= a_{f0} + a_{f1}(t - t_0) + a_{f2}(t-t_0)^2 + \Delta t_r$
Δt_r	$= Fe\sqrt{a}\sin(E_k)$
$\rho_{corrected}$	= pseudorange corrected for SV clock error
ρ	= pseudorange
$c\Delta t_{sv}$	= SV clock correction
$a_{f0}, a_{f1}, a_{f2}, t_0$	= SV clock correction parameters from navigation message
Δt_r	= relativity correction (since not circular orbit)
F	= constant = $-4.442807633 \times 10^{-10}$ sec/(meter)$^{1/2}$
e	= eccentricity from navigation message
$\sqrt{a}$	= square root of semi-major axis from navigation message
E_k	= Eccentric anomaly (from SV position calculation)

Stand-alone GPS positioning techniques are fast and reliable. However, the poor accuracy results (typically 30-50 m) are undesirable. In order to obtain the relative

accuracy required for vehicle formation flying, kinematic and DGPS techniques must be employed.
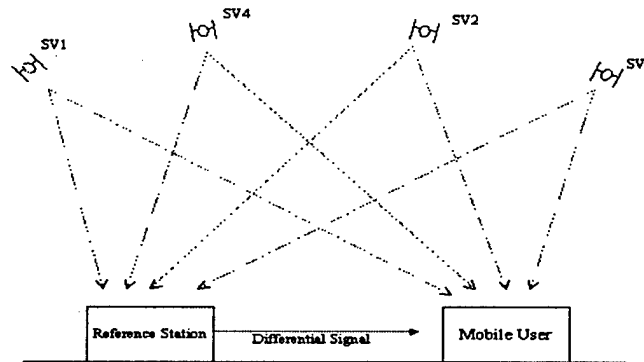
Figure 2.   Typical DGPS Situation

2.2.2   *Differential GPS Positioning Techniques*

The principal idea behind DGPS is that, because a reference receiver's position is known, common errors between it and relatively close mobile receivers can be removed. Generally, there are two basic DGPS techniques; code and carrier-phase based.

2.2.2.1   *Code Based Algorithm*

Let the reference receiver, *m*, have a known position represented as (x_m, y_m, z_m) and the reported i^{th} satellite position (via ephemeris data) be represented as (x_i, y_i, z_i). The geometric distance from the reference receiver to the ith satellite is known and can be represented as

$$R_m^i = \sqrt{(x_i - x_m)^2 + (y_i - y_m)^2 + (z_i - z_m)^2} \qquad (2\text{-}13)$$

The reference receiver is then able to generate a pseudorange measurement to the ith

satellite as

$$\rho_m^i = R_m^i + \varepsilon_{m,space} + \varepsilon_{m,user} + c\delta t_m \qquad (2\text{-}14)$$

where $\varepsilon_{m,space}$, $\varepsilon_{m,control}$ and $\varepsilon_{m,user}$ are the space, control, and user segment induced

pseudorange errors respectively, and $c\delta t_m$ is the reference receiver's clock offset from

GPS time. The errors are summarized in Table 1 [6]. The reference receiver simply

resolves the difference between the generated pseudorange to the ith satellite, ρ_m^i and it's

geometric range, R_m^i, to create the desired correction term.

$$\Delta\rho_m^i \overset{\Delta}{=} \rho_m^i - R_m^j = \varepsilon_{m,space} + \varepsilon_{m,control} + \varepsilon_{m,user} + c\delta t \qquad (2\text{-}15)$$

This correction term utilized by the user, or mobile, receiver where it is differenced

with the users' generated pseudorange measurement to the *same* satellite is

$$\rho_u^i - \Delta\rho_m^i = R_u^j + \varepsilon_{u,space} + \varepsilon_{u,control} + \varepsilon_{u,user} + c\delta t \dots$$
$$\dots - (\varepsilon_{m,space} + \varepsilon_{m,control} + \varepsilon_{m,user} + c\delta t) \qquad (2\text{-}16)$$

If the user's receiver is located relatively nearby the reference receiver, the user's

receiver pseudorange equation error components will be nearly identical to those of the

reference receiver. Exceptions include errors that are not common to both receivers, i.e.,

multi-path and receiver noise. Therefore, the corrected user pseudorange is obtained as

$$\rho_{u,corrected} = R_u^j + \varepsilon_u' + c\delta t_{combined} \qquad (2\text{-}17)$$

where ε_u' is the *residual* user segment error (multi-path, etc) and $\delta t_{combined}$ is the combined

clock offset. A typical comparison between stand-alone measurements and DGPS

measurements is given in Table 1 [6].

Table 1. Typical Satellite errors before/after DGPS correction

Segment Source	Error Source	GPS 1σ Error (m)	Typical GPS 1σ errors after DGPS corrections
Space	Satellite clock stability	3.0	0
	Satellite perturbation	1.0	0
	Selective Availability	32.3	0
	Other (thermal, radiation, etc)	0.5	0
Control	Ephemeris prediction error	4.2	0
	Other (thruster performance, etc)	0.9	0
User	Ionospheric delay	5.0	0
	Tropospheric delay	1.5	0
	Receiver noise and resolution	1.5	2.1
	Multipath	2.5	2.5
	Other (inter-channel bias, etc)	0.5	0.5
System UERE	Total (rms)	33.3	3.3

2.2.2.2 Carrier-Phase Based Algorithm

Obviously, more precise position information can be obtained by measuring the

amount of shift in the frequency (Doppler shift) of the received signal. This shift in

carrier frequency arises from the relative motion of the GPS satellites to the user

resulting in Doppler shift frequencies of $\Delta f = \pm 5000\,Hz$. Thus,

$$\Delta f = f_R - f_T \qquad (2\text{-}18)$$

where,

$$f_R \quad = \text{Frequency received at the receiver}$$
$$f_T \quad = \text{Known transmitted frequency}$$

Integration of the Doppler shift offset over time can result in extremely precise

measurements (centimeter range for the L1 and L2 frequencies). Thus, the carrier phase

measurements, $\phi(t)$, can be calculated by integrating the Doppler measurements over the time epoch:

$$\phi(t) = \int_0^t \Delta f_{meas}(t)dt + \phi(t_0) \qquad (2\text{-}19)$$

The integer portion of the initial carrier-phase at the start of the integration, $\phi(t)$, is referred to as the "carrier-phase integer ambiguity." This integer-ambiguity exists because the receiver merely begins counting carrier cycles once the user tracks the satellite signal. Resolution of this integer ambiguity is paramount in determining the most precise range measurement possible. Several techniques have been utilized to resolve this problem, most popular of which are the least-squares iteration process or LAMBDA methods [3, 7, 10].

2.2.3 General Kinematic GPS Techniques

In some of the less advanced receivers, user velocity is calculated as the time derivative of the estimated position, i.e.

$$\dot{u} = \frac{du}{dt} \approx \frac{u(t_2) - u(t_1)}{t_2 - t_1} \qquad (2\text{-}20)$$

In general, this approach yields poor results and is acceptable only if the user's velocity is constant over the selected time interval.

Many receivers process carrier phase measurements, which effectively estimate the Doppler frequency of the received satellite. The satellite velocity vector is computed using the ephemeris data and an orbital model that resides within the receiver [6]. At the

2-9

receiver antenna, the received frequency, f_R, is given by the classical Doppler equation

(neglecting relativistic effects) as follows

$$f_R = f_T (1 - \frac{(\mathbf{v}_r \cdot \mathbf{a})}{c})$$

(2-21)

where,

f_T = transmitted satellite signal frequency (known)
$\mathbf{v}_r$ = satellite-to-user relative velocity vector
$\mathbf{a}$ = is the unit vector pointing along the line of sight from the user to the satellite
c = speed of light

The dot product represents the radial component of the satellite-user relative velocity

vector along the instantaneous line of sight to the satellite vector, a_r. The quantity v_r is

given as the velocity difference

$$\mathbf{v}_r = \mathbf{v} - \dot{\mathbf{u}}$$

(2-22)

where $\mathbf{v}$ is the (known) velocity of the satellite and $\dot{\mathbf{u}}$ is the velocity of the user to be

determined (both referenced to a common ECEF frame). Therefore, the Doppler offset

due to the relative motion satisfies

$$\Delta f = f_R - f_T = -f_T \frac{(\mathbf{v} - \dot{\mathbf{u}}) \cdot \mathbf{a}}{c}$$

(2-23)

There are several techniques to obtain user velocity, $\mathbf{u}$, from the measured Doppler

frequency, Δf.

For the jth satellite, equation (2-23) yields

$$f_{R_j} = f_{T_j} \left\{ 1 - \frac{1}{c} [(\mathbf{v}_j - \dot{\mathbf{u}}) \cdot \mathbf{a}_j] \right\}$$

(2-24)

and the corrected satellite frequency is given by

$$f_{T_j} = f_o + \Delta f_{T_j} \tag{2-25}$$

where f_o is the nominal transmitted frequency (L1 or L2) and Δf_{T_j} is the correction

determined from the navigation message update.

The measured value of the received frequency is in error due to the frequency bias

offset. This offset is related to the drift rate of the user clock, relative to GPS time, by

$$f_{R_j} = f_j (1 + \delta t_u) \tag{2-26}$$

where δt_u is considered positive if the user clock is running fast. Through algebraic

manipulation, this can be rewritten as

$$\frac{c(f_j - f_{T_j})}{f_{Tj}} + v_{xj} a_{xj} + v_{yj} a_{yj} + v_{zj} a_{zj} = \dot{x}_u a_{xj} + \dot{y}_u a_{yj} + \dot{z}_u a_{zj} - \frac{c f_j \delta t}{f_{Tj}} \tag{2-27}$$

where $\mathbf{v}_j$, $\mathbf{a}_j$ is the jth satellite velocity and acceleration component respectively and

$\dot{x}_u, \dot{y}_u, \dot{z}_u$ is the user velocity, $\mathbf{V}$. To simplify this equation, we let

$$d_j = \frac{c(f_j - f_{Tj})}{f_{Tj}} + v_{xj} a_{xj} + v_{yj} a_{yj} + v_{zj} a_{zj} \tag{2-28}$$

Since the term f_j / f_{T_j} is $\cong 1$, the equation can be written as

$$d_j = \dot{x}_u a_{xj} + \dot{y}_u a_{yj} + \dot{z}_u a_{zj} - c\delta t \tag{2-29}$$

We now have four unknowns that can be solved for by using measurements from four

satellites and using a set of linear equations, i.e.,

$$d = \begin{bmatrix} d_1 \\ d_2 \\ d_3 \\ d_4 \end{bmatrix} \quad H = \begin{bmatrix} a_{x1} & a_{y1} & a_{z1} & 1 \\ a_{x2} & a_{y2} & a_{z2} & 1 \\ a_{x3} & a_{y3} & a_{z3} & 1 \\ a_{x4} & a_{y4} & a_{z4} & 1 \end{bmatrix} \quad g = \begin{bmatrix} \dot{x}_u \\ \dot{y}_u \\ \dot{z}_u \\ -c\delta t_u \end{bmatrix} \tag{2-30}$$

with the general form

$$\mathbf{d} = \mathbf{Hg} \qquad (2\text{-}31)$$

which can be solved as

$$\mathbf{g} = \mathbf{H}^{-1}\mathbf{d} \qquad (2\text{-}32)$$

The previously stated technique for obtaining user velocity, equation (2-32), uses measurements that may be corrupted by (measurement) noise and/or multi-path errors. A Kalman Filter method may be used to compute a smoothed navigation solution.

The Kalman filter technique is a recursive algorithm that provides optimum estimates of user position, velocity and clock drift (PVT) based on noise statistics and current measurements. The filter contains a kinematic model of the GPS receiver platform and outputs a set of user receiver position and velocity state estimates as well as the associated error variances. Kalman Filters entail an approach which simultaneously estimates eight states: 3 position states, 3 velocity states, 1 receiver clock bias and 1 receiver clock drift. In general, the velocity estimates are only valid for low dynamic situations.

Generally, the dynamical model can be derived from a Taylor series expansion

$$\mathbf{u}(t) = \mathbf{u}(t_0) + \frac{d\mathbf{u}(t)}{dt}\Big|_{t=t_0}(t-t_0) + \frac{1}{2!}\frac{d\mathbf{u}^2(t)}{dt^2}\Big|_{t=t_0}(t-t_0)^2 + \ldots$$
$$\ldots + \frac{1}{3!}\frac{d\mathbf{u}^3(t)}{dt^3}\Big|_{t=t_0}(t-t_0)^3 + h.o.t \qquad (2\text{-}33)$$

In summary, the filter propagates the platform position from one time point to the next. Using these propagated states, the receiver calculates the anticipated pseudorange

and delta pseudorange (the change in pseudorange per epoch for each satellite). Next, the pseudorange and delta pseudoranges are measured and the difference between the anticipated and the measured values (residuals or errors in the user position and velocity estimates) is taken. These errors are usually sent back through the algorithm to be utilized in future state estimates.

Utilizing a Kalman filter allows the use of fewer then 4 satellites and adjusts the state estimates to weight the effects of measurement noise. That is, when measurement noise is high, the filter places heavier weights on the state estimates while, on the other hand, the filter places heavier weights on the measurements when the noise is low.

2.3 Summary

This chapter described the conventional GPS techniques used to determine user position and velocity. The use of DGPS techniques allows the removal of nearly all common errors in each of the three segments (User, Control, and Space) as can be seen in Table 1. However, errors that are uncorrelated from receiver to receiver are not removed and, in particular, the receiver measurement noise is actually increased. In addition, the theory behind the new algorithm is described.

3 Novel DGPS Position-Velocity Estimation Algorithm

3.1 Overview

This chapter provides a detailed description of the novel algorithm developed to estimate user position and velocity. Only pseudorange measurements are used.

3.2 Problem Statement

Two or more mobile users are considered over a pre-specified short time interval. The number and the specific GPS satellites in view of the users' platforms is held constant during the measurement interval.

At the beginning of the time interval, prior information on user 2's position (and velocity) is available. Pseudorange data is collected over several epochs during the measurement interval; a fixed sample rate is used. The prior information and all pseudorange measurements are processed simultaneously at the end of the measurement interval and estimates of the position and velocity of both users 1 and 2 are obtained. The effect of having varying degrees of uncertainty in the user 2's "reference station" prior position information is examined. Additionally, the effect of receiver noise on the algorithm's ability to correctly estimate the users' position and velocity in the face of user and satellite clock errors is investigated.

3.3 Theory

The developed novel algorithm integrates kinematic modeling and differential GPS. This is achieved by maximizing the use of the information in the pseudorange measurements from n satellites that are available at $N+1$, relatively close, time instants during the measurement interval. The correct treatment of the common errors, and

proper stochastic modeling of the measurement situation on hand, are responsible for achieving improved user positioning.

A sampling interval of ΔT seconds is used. The duration, T, of the measurement interval consists of $N+1$ discrete measurement epochs. Thus, the time instants when measurements are taken are

$$t_j = \Delta T \cdot j \qquad (3\text{-}1)$$

where

$$j = 0, 1, ..., N \qquad (3\text{-}2)$$

Hence, the number of epochs available over the duration of the measurement interval is $N+1$ where

$$N = \frac{T}{\Delta T}. \qquad (3\text{-}3)$$

For the short measurement duration, T, being investigated, the users' kinematics are modeled as constant speed and rectilinear motion, viz.,

$$\vec{x}_k(t) = \vec{x}_{0_k} + \vec{V}_k \cdot t \qquad (3\text{-}4)$$

where $k = 1, 2, ..., m$ and m is the number of users and $\vec{x}_k, \vec{x}_{0_k}, \vec{V}_k \in \Re^3$.

The kinematic model could include higher order terms such as acceleration, jerk or, more importantly, could represent a more complex motion (i.e., a satellite trajectory parameterized by its orbital parameters). However, for the generic scenario examined, equation (3-4) will be the kinematic model chosen for the users' motion.

The pseudorange from the kth user to the ith satellite measured at time t is modeled as

$$Z_i^{(k)} = \rho_i^{(k)}(t) + v_i^{(k)}(t) \qquad (3\text{-}5)$$

where the pseudorange

$$\rho_i^{(k)}(t) = \sqrt{\left[x_k(t) - x_{s_i}(t)\right]^2 + \left[y_k(t) - y_{s_i}(t)\right]^2 + \left[z_k(t) - z_{s_i}(t)\right]^2} + \tau_k + \tau_{s_i} \qquad (3\text{-}6)$$

and

$v_i^{(k)}(t)$ is the measurement noise in the ith channel of user k^{th} receiver at time t.

τ_k is the kth user range equivalent clock bias.

τ_{s_i} is the ith satellite range-equivalent clock bias.

$(x_{s_i}, y_{s_i}, z_{s_i})$ is the ith satellite position from the ephemeris data.

(x_k, y_k, z_k) is the kth user position at time t, k=1, 2, ..., m.

i is the satellite number (number of satellites in view is n).

The measurement noise at time j is modeled as

$$v_{i,j}^{(k)} = N(0, \sigma^2) \qquad (3\text{-}7)$$

and

$$E(v_{i,j}^{(k)} \cdot v_{i',j'}^{(k')}) = 0 \quad for \ i \neq i', j \neq j' \ or \ k \neq k'. \qquad (3\text{-}8)$$

Incorporating the kinematic modeling of Equation (3-4) for the users positions for each

time instant, i.e., setting

$$
\begin{aligned}
x_k(t) &\to x_{0_k} + (V_{k_x} \cdot \Delta T)j \\
y_k(t) &\to y_{0_k} + (V_{k_y} \cdot \Delta T)j \\
z_k(t) &\to z_{0_k} + (V_{k_z} \cdot \Delta T)j
\end{aligned}
\qquad (3\text{-}9)
$$

where the subscript '0' denotes the initial position at time t=0 (j=0) and

$$j = 0, 1, ..., N, \qquad (3\text{-}10)$$

allows Equation (3-6) to be written as

$$
\rho_{i,j}^{(k)} = \sqrt{\left[x_{0_k} + (V_{k_x} \cdot \Delta T)j - x_{s_i}(t)\right]^2 + \left[y_{0_k} + (V_{k_y} \cdot \Delta T)j - y_{s_i}(t)\right]^2 \atop + \left[z_{0_k} + (V_{k_z} \cdot \Delta T)j - z_{s_i}(t)\right]^2} + \tau_k + \tau_{s_i}
\qquad (3\text{-}11)
$$

Note that in Equation (3-11), $t = j\Delta T$.

The parameter vector of interest is

$$\theta = \begin{pmatrix} x_{0_1} \\ y_{0_1} \\ z_{0_1} \\ V_{x_1}\Delta T \\ V_{y_1}\Delta T \\ V_{z_1}\Delta T \\ x_{0_2} \\ y_{0_2} \\ z_{0_2} \\ V_{x_2}\Delta T \\ V_{y_2}\Delta T \\ V_{z_2}\Delta T \\ \tau_1 \\ \tau_2 \\ \tau_{s_1} \\ \tau_{s_2} \\ \tau_{s_3} \\ \tau_{s_4} \\ \tau_{s_5} \end{pmatrix} \qquad (3\text{-}12)$$

where

$(x_{0_k}, y_{0_k}, z_{0_k})$ is the kth user initial ($t = 0$) ECEF coordinates, k = 1, 2,...,m.

$(V_{x_k}, V_{y_k}, V_{z_k})$ is the kth user velocities, k = 1, 2, ..., m.

τ_k represents the kth users range-equivalent receiver clock error, k = 1, 2,...,m.

τ_{s_i} represents the ith satellite range-equivalent clock error, i = 1, 2, ..., n.

In the case where two users (m=2) and five (n=5) satellites are considered, the parameter

vector is shown in Equation (3-12) and $\theta \in \Re^{19}$. In the general case, the parameter

$$\theta \in \Re^{7m+n} \qquad (3\text{-}13)$$

In the algorithm, the pseudoranges received are composed systematically. First, the pseudoranges received by the kth user from n satellites at time instant j are used to form the n x 1 vector

$$Z_j^{(k)} = \begin{pmatrix} \rho_{1,j}^{(k)} \\ \vdots \\ \rho_{n,j}^{(k)} \end{pmatrix} \qquad (3\text{-}14)$$

Now, composing the received pseudoranges over the $N+1$ time instants yields the $n(N+1)$x1 vector

$$Z^{(k)} = \begin{pmatrix} Z_0^{(k)} \\ \vdots \\ Z_N^{(k)} \end{pmatrix} \qquad (3\text{-}15)$$

and finally, composing for the m users yields the $mn(N+1)$x1 "measurement" vector

$$Z = \begin{pmatrix} Z^{(1)} \\ \vdots \\ Z^{(m)} \end{pmatrix} \qquad (3\text{-}16)$$

The pseudorange information, $\rho(\theta)$, is composed similarly: Defining

$$f_{i,j}^{(k)}(\theta) = \sqrt{\left[x_{0_k} + (V_{x_k} \cdot \Delta T)j - x_{s_i}(t)\right]^2 + \left[y_{0_k} + (V_{y_k} \cdot \Delta T)j - y_{s_i}(t)\right]^2 + \ldots \ldots + \left[z_{0_k} + (V_{z_k} \cdot \Delta T)j - z_{s_i}(t)\right]^2} \qquad (3\text{-}17)$$

and

$$\rho_{i,j}^{(k)}(\theta) = f_{i,j}^{(k)}(\theta) + \tau_k + \tau_{s_i} \qquad (3\text{-}18)$$

we compose

$$f_j^{(k)} = \begin{pmatrix} f_{1,j}^{(k)} \\ \vdots \\ f_{n,j}^{(k)} \end{pmatrix} \qquad (3\text{-}19)$$

Next, composing the *N+1* time epochs we obtain

$$f^{(k)} = \begin{pmatrix} f_0^{(k)} \\ \vdots \\ f_N^{(k)} \end{pmatrix} \qquad (3\text{-}20)$$

and finally, composing for the *m* users yields

$$f = \begin{pmatrix} f^{(1)} \\ \vdots \\ f^{(m)} \end{pmatrix} \qquad (3\text{-}21)$$

The vector *f* is *mn(N+1)x1*. The vector ρ is similarly composed, thus obtaining the

function $\rho(\theta)$: $\Re^{7m+n} \rightarrow \Re^{mn(N+1)}$.

The (nonlinear) GPS equations are

$$Z = \rho(\theta) + W \qquad (3\text{-}22)$$

where the mn(N+1) equation error vector W represents the composed measurement noise

$$W = \begin{pmatrix} v_{1,0}^{(1)} \\ \vdots \\ v_{n,N}^{(m)} \end{pmatrix}_{mn(N+1)x1} \qquad (3\text{-}23)$$

with covariance

$$R_1 = E(W \cdot W^T) = \sigma^2 I_{mn(N+1)} \qquad (3\text{-}24)$$

Linearization with respect to the parameter θ, at the lth iteration, about the current

parameter estimate $\hat{\theta}^{(l)}$, yields

$$Z=\rho(\hat{\theta}^{(l)})+\left.\frac{\partial\rho}{\partial\theta}\right|_{\theta=\hat{\theta}^{(l)}}(\theta-\hat{\theta}^{(l)})+W \tag{3-25}$$

Equation (3-25) is rearranged to yield the linear regression in θ

$$Z+\left.\frac{\partial\rho}{\partial\theta}\right|_{\theta=\hat{\theta}^{(l)}}\cdot\hat{\theta}^{(l)}-\rho(\hat{\theta}^{(l)})=\left.\frac{\partial\rho}{\partial\theta}\right|_{\theta=\hat{\theta}^{(l)}}\theta+W \tag{3-26}$$

Now, the calculation of the regressor matrix requires the composition of the partials of $\rho(\theta)$ with respect to the parameter vector θ, i.e.

$$H_{i,j}^{(k)}(\theta)=\frac{\partial\rho_{i,j}^{(k)}(\theta)}{\partial\theta} \tag{3-27}$$

$H_{i,j}^{(k)}$ is an $1\text{x}(7m+n)$ row vector. Its entries are explicitly given by

$$H_{i,j}^{(k)}(\theta)=\frac{1}{f_{i,j}^{(k)}(\theta)}\left[\theta^{T}\cdot E_{i,k}(j)-x_{s_{i,j}}e_{1_{i,k}}(j)-y_{s_{i,j}}e_{2_{i,k}}(j)-z_{s_{i,j}}e_{3_{i,k}}(j)\right]+e_{i,k} \tag{3-28}$$

where

$(x_{s_{i,k}}, y_{s_{i,k}}, z_{s_{i,k}})$ is the ith satellite position at time j.

$e_{i,k}(j), e_{1_{i,k}}(j), e_{2_{i,k}}(j), e_{3_{i,k}}(j)$ are $7m+4n$ row vectors of zeros with 1's, j, and j^2 located at positions indicated in their subscripts, according to:

$e_{1_{i,k}}(j)=e_{7k-6,7k-3,7m+4i-3}$ $\qquad$ $e_{2_{i,k}}(j)=e_{7k-5,7k-2,7m+4i-2}$

$e_{3_{i,k}}(j)=e_{7k-9,7k-1,7m+4i-1}$ $\qquad$ $e_{i,k}=e_{7k,7m+4i}$,

and the matrix

$$E_{i,k}(j)=e_{1_{i,k}}^{T}e_{1_{i,k}}+e_{2_{i,k}}^{T}e_{2_{i,k}}+e_{3_{i,k}}^{T}e_{3_{i,k}}. \tag{3-29}$$

The composition of the regressor matrix is analogous to the process employed for Z and f.

First, for the n satellites, the $n\text{x}(7m+n)$ matrix

$$H_j^{(k)}(\theta)=\begin{pmatrix} H_{1,j}^{(k)}(\theta) \\ \vdots \\ H_{n,j}^{(k)}(\theta) \end{pmatrix} \qquad (3\text{-}30)$$

is formed, followed by composition over the $N+1$ time epochs, yielding the

$n(N+1)$x$(7m+n)$ matrix

$$H^{(k)}(\theta)=\begin{pmatrix} H_0^{(k)}(\theta) \\ \vdots \\ H_N^{(k)}(\theta) \end{pmatrix} \qquad (3\text{-}31)$$

Finally, for the m users, the $mn(N+1)$x$(7m+n)$ regressor matrix

$$H(\theta)=\begin{pmatrix} H^{(1)}(\theta) \\ \vdots \\ H^{(m)}(\theta) \end{pmatrix} \qquad (3\text{-}32)$$

is formed. Thus, Equation (3-26) yields

$$Z+\left.\frac{\partial f}{\partial \theta}\right|_{\theta=\hat{\theta}^{(l)}}\cdot\hat{\theta}^{(l)}-f(\hat{\theta}^{(l)}) = \left.\frac{\partial \rho}{\partial \theta}\right|_{\theta=\hat{\theta}^{(l)}}\theta + W$$
$$=H(\hat{\theta}^{(l)})\theta + W \qquad (3\text{-}33)$$

The function $\rho(\theta): \Re^{7m+n} \to \Re^{mn(N+1)}$ is linear in the users' and satellites' clock error

parameters and therefore the function $\rho(\theta)$ is replaced by the function $f(\theta)$ in the left

hand side of Equation (3-33).

The solution for the users' "positions", viz., θ, can be obtained using least squares,

whereupon, the Iterated Least Squares (ILS) algorithm is established:

$$\hat{\theta}^{(l+1)}=(H^T(\hat{\theta}^{(l)})\cdot H(\hat{\theta}^{(l)}))^{-1}(H(\hat{\theta}^{(l)}))^T[Z+\left.\frac{\partial f}{\partial \theta}\right|_{\theta=\hat{\theta}^{(l)}}\cdot\hat{\theta}^{(l)}-f(\hat{\theta}^{(l)})] \qquad (3\text{-}34)$$

where

Z is the received 'stacked up' pseudorange measurements $mn(N+1)x1$ vector according to Equation (3-16)

f is the $mn(N+1)x1$ vector of ranges calculated according to Equation (3-17)

H is the $mn(N+1)x(7m+n)$ regressor matrix formed from the partials of ρ according to Equation (3-32).

3.3.1 Reduced parameter vector

The regressor H is further examined. As stated in equation (3-12), the parameter vector contains $7m+n$ variables: 3 positions, 3 velocities and a clock bias variable for each of the two (m=2) users, as well as the five (n=5) satellite clock error terms (19 variables in total). The main objective of the algorithm is to solve for the (non-reference) users' position and velocity rather than the users' and satellites' clock biases. Hence, the regressor's matrix, $H(\hat{\theta}^{(l)})$, structure is examined and the algorithm is modified according to the following analysis.

We define the $mn(N+1)x(m+n)$ matrix

$$\mathbf{B}=[\mathbf{b}_1,\mathbf{b}_2,...,\mathbf{b}_m,\gamma_1,\gamma_2,...\gamma_n] \tag{3-35}$$

where

$\mathbf{b}_k$ is the column of H operating on user k's clock variable, $k = 1, 2, ..., m$

γ_i is the H column operating on the ith satellite clock variable, $i = 1, 2, ..., n$

Indeed, the structure of the regressor matrix $H(\hat{\theta}^{(l)})$ is

$$H =[Diag(\tilde{H}^{(k)}(\hat{\theta}^{(l)})) \vdots B] \tag{3-36}$$

where the $n(N+1)x6$ matrices $\tilde{H}^{(k)}$ are the $H^{(k)}$ matrices with only the six columns 6k-5, ..., 6k retained. In the case where m=2, and therefore, k=1, 2,

$$H = \begin{bmatrix} \tilde{H}^{(1)}(\hat{\theta}^{(l)}) & 0 \\ 0 & \tilde{H}^{(2)}(\hat{\theta}^{(l)}) & B \end{bmatrix} \tag{3-37}$$

where the $\tilde{H}^{(1)}$ and $\tilde{H}^{(2)}$ matrices are given by the partials of f in (x_{0_1}, y_{0_1}, z_{0_1}, $V_{x_1}\Delta T$,

$V_{y_1}\Delta T$, $V_{z_1}\Delta T$) and (x_{0_2}, y_{0_2}, z_{0_2}, $V_{x_2}\Delta T$, $V_{y_2}\Delta T$, $V_{z_2}\Delta T$), respectively. The matrix

$$B = \begin{bmatrix} & & I_n \\ Diag(e_{N+1}) & \vdots \\ & & I_n \end{bmatrix} \tag{3-38}$$

where

e_{N+1} is a vector of ones of size *(N+1)* x *1*
I_n is an identity matrix of size n

For example, for m=2

$$B = \begin{bmatrix} e_{N+1} & 0 & I_n \\ & & \vdots \\ 0 & e_{N+1} & I_n \end{bmatrix} \tag{3-39}$$

The following holds

$$\sum_{k=1}^{m} b_k = \sum_{i=1}^{n} \gamma_i \tag{3-40}$$

Evidently, the matrix B (and therefore the regressor H) is rank deficient. Thus perform

the full rank factorization of B,

$$B = B_1 K \tag{3-41}$$

where B_1 is a full rank *(m+n-1)*, *mn(N+1)x(m+n-1)* matrix of the form

$$B_1 = \begin{bmatrix} b_1, ..., b_{m-1}, \sum_{k=1}^{m} b_k, \gamma_1, ..., \gamma_{n-1} \end{bmatrix} \tag{3-42}$$

In the case where $m=2$

$$B_1 = [b_1, b_1 + b_2, \gamma_1, ..., \gamma_{n-1}] \qquad (3\text{-}43)$$

Therefore, solving Equation (3-41) for K yields the blocked $(m+n-1)x(m+n)$ matrix

$$K = \begin{bmatrix} A & B & C \\ D & E & F \end{bmatrix} \qquad (3\text{-}44)$$

where

$$A = \begin{bmatrix} I_{m-1} & -e_{m-1} \\ 0_{1x(m-1)} & 1 \end{bmatrix}, \quad B = 0_{mx(n-1)}, \quad C = \begin{bmatrix} 0_{(m-1)x1} \\ 1 \end{bmatrix} \qquad (3\text{-}45)$$

$$D = 0_{(n-1)xm}, \qquad E = I_{n-1}, \qquad F = -e_{n-1}$$

where
> 0 is a zero matrix
> e_n is a vector of ones of length n

Next, partition the regressor

$$H = [\tilde{H} \vdots B] \qquad (3\text{-}46)$$

where $\tilde{H} = Diag(\tilde{H}^{(k)})$ is a $mn(N+1)x6m$ matrix consisting of the columns operating on

the users' position and velocity parameters only. Also define the reduced, full rank,

matrix

$$H_1 = [\tilde{H} \vdots B_1]. \qquad (3\text{-}47)$$

Next, perform the full rank factorization of the regressor H

$$H = H_1 K_1, \qquad (3\text{-}48)$$

i.e., the following equation is solved for the $(7m+n-1)x(7m+n)$ matrix K_1:

$$[\tilde{H} \vdots B_1 K] = [\tilde{H} \vdots B_1] \cdot K_1 \qquad (3\text{-}49)$$

We calculate:

$$K_1 = \begin{bmatrix} I_{(6m) \times (6m)} & \Theta_{(6m) \times (m+n)} \\ \Theta_{(m+n-1) \times 6m} & K_{(m+n-1) \times (m \times n)} \end{bmatrix}$$

(3-50)

Finally, the reduced parameter vector is defined,

$$\theta_1 = K_1 \theta$$

(3-51)

where θ is as specified in Equation (3-12) and the reduced parameter

vector $\theta_1 \in \Re^{7m+n-1}$ consists of the users' position and velocity parameters as well as linear

combinations of the user and satellite clock biases. For the specific scenario examined in

which we have 2 mobile users and 5 satellites visible, this yields

$$\theta_1 = \begin{pmatrix} x_{0_1} \\ y_{0_1} \\ z_{0_1} \\ V_{x1}\Delta T \\ V_{y1}\Delta T \\ V_{z1}\Delta T \\ x_{0_2} \\ y_{0_2} \\ z_{0_2} \\ V_{x2}\Delta T \\ V_{y2}\Delta T \\ V_{z2}\Delta T \\ \tau_1 - \tau_2 \\ \tau_2 + \tau_{s5} \\ \tau_{s1} - \tau_{s5} \\ \tau_{s2} - \tau_{s5} \\ \tau_{s3} - \tau_{s5} \\ \tau_{s4} - \tau_{s5} \end{pmatrix}_{18 \times 1}$$

(3-52)

Since

$$H\theta = H_1 K_1 \theta = H_1 \theta_1 \tag{3-53}$$

Equation (3-33) is written with the reduced parameter:

$$Z + H_2(\hat{\theta}_2^{(l)}) \cdot \hat{\theta}_2^{(l)} - f(\hat{\theta}_2^{(l)}) = H_1(\hat{\theta}_2^{(l)}) \cdot \theta_1 + W \tag{3-54}$$

where

$$\theta_2 = \begin{pmatrix} x_{0_1} \\ y_{0_1} \\ z_{0_1} \\ V_{x_1} \Delta T \\ V_{y_1} \Delta T \\ V_{z_1} \Delta T \\ x_{0_2} \\ y_{0_2} \\ z_{0_2} \\ V_{x_2} \Delta T \\ V_{y_2} \Delta T \\ V_{z_2} \Delta T \end{pmatrix} \tag{3-55}$$

Hence, θ_2 is stripped of the clock error parameters of θ_1 and is used in the left hand side of Equation (3-54) (not θ_1) because the function ρ is linear in the time parameters. H_2 is composed of the first $6m$ columns H associated with the parameters featuring in θ_2 (positions and velocities, and no clock biases). Thus, $H_2 = Diag(\tilde{H}^{(k)})$.

Finally, the linear regression is augmented to include the prior information on user 2 (position and velocity). The prior information is provided in the form

$$x_{0_2} = N(\bar{x}_{0_2}, \sigma^2_{x_{0_2}})$$

$$y_{0_2} = N(\bar{y}_{0_2}, \sigma^2_{y_{0_2}})$$

$$z_{0_2} = N(\bar{z}_{0_2}, \sigma^2_{z_{0_2}})$$

$$V_{x_2} = N(\bar{V}_{x_2}, \sigma^2_{V_{x_2}})$$ (3-56)

$$V_{y_2} = N(\bar{V}_{y_2}, \sigma^2_{V_{y_2}})$$

$$V_{z_2} = N(\bar{V}_{z_2}, \sigma^2_{V_{z_2}})$$

This enables the augmentation of the linear regression in Equation (3-54). The linear regression is augmented as follows. The vector Z is augmented in Equation (3-57):

$$Z := \begin{pmatrix} Z \\ \cdots \\ Z_1 \end{pmatrix}$$ (3-57)

where

$$Z_1 = \begin{pmatrix} \bar{x}_{0_2} \\ \bar{y}_{0_2} \\ \bar{z}_{0_2} \\ \bar{V}_{x_2} \\ \bar{V}_{y_2} \\ \bar{V}_{z_2} \end{pmatrix}$$ (3-58)

In addition,

$$H_1 := \begin{pmatrix} H_1 \\ \cdots \\ M_1 \end{pmatrix}$$ (3-59)

where the $6x(7m+n-1)$ selector matrix M_1 is

$$M_1 = \begin{bmatrix} 0_{6x6} & \vdots & I_6 & \vdots & 0_{6x6} \end{bmatrix}$$ (3-60)

and when added to H_1 picks out the $x_{0_2}, y_{0_2}, z_{0_2}, V_{x_2}\Delta T, V_{y_2}\Delta T, V_{z_2}\Delta T$ elements of the

parameter vector θ_1. Finally,

$$H_2 := \begin{pmatrix} H_2 \\ \cdots \\ M_2 \end{pmatrix} \qquad (3\text{-}61)$$

where

$$M_2 = 0_{6x12}, \qquad (3\text{-}62)$$

$$f := \begin{pmatrix} f \\ \cdots \\ 0_{6x1} \end{pmatrix} \qquad (3\text{-}63)$$

and

$$W = \begin{pmatrix} W \\ \cdots \\ W_{mn(N+1)+1} \\ \vdots \\ W_{mn(N+1)+6} \end{pmatrix} \qquad (3\text{-}64)$$

Additionally, a weighting matrix, R, is included, similar to equation (2-9), to correctly

incorporate the confidence levels in the "reference" receiver's (user #2) position and

velocity, and, possibly, clock bias prior information. This finally yields

$$\hat{\theta}_1^{(l+1)} = (H_1^T(\hat{\theta}_2^{(l)}) \cdot R^{-1} H_1^T(\hat{\theta}_2^{(l)}))^{-1}(H_1(\hat{\theta}_2^{(l)}))^T R^{-1}[Z + H_2(\hat{\theta}_2^{(l)}) \cdot \hat{\theta}_2^{(l)} - f(\hat{\theta}_2^{(l)})] \quad (3\text{-}65)$$

where R is a *[nm(N+1)+6]* x *[nm(N+1)+6]* diagonal matrix

$$R = Diag(R_1, R_2), \qquad (3\text{-}66)$$

and where

$$R_1 = \sigma^2 \cdot I_{mn(N+1)} \tag{3-67}$$

is determined by the measurement noise variance σ and the diagonal R_2 contains the

standard deviations of the reference station's position and velocity prior information, viz.,

$$R_2 = \begin{pmatrix} \sigma^2_{x_{0_2}} & 0 & 0 & 0 & 0 & 0 \\ 0 & \sigma^2_{y_{0_2}} & 0 & 0 & 0 & 0 \\ 0 & 0 & \sigma^2_{z_{0_2}} & 0 & 0 & 0 \\ 0 & 0 & 0 & \sigma^2_{V_{x_2}} & 0 & 0 \\ 0 & 0 & 0 & 0 & \sigma^2_{V_{y_2}} & 0 \\ 0 & 0 & 0 & 0 & 0 & \sigma^2_{V_{z_2}} \end{pmatrix}_{6x6} \tag{3-68}$$

where

$$\sigma^2_{x_{0_2}} = E(W^2_{mn(N+1)+1})$$

$$\sigma^2_{y_{0_2}} = E(W^2_{mn(N+1)+2})$$

$$\sigma^2_{z_{0_2}} = E(W^2_{mn(N+1)+3})$$

$$\sigma^2_{V_{x_2}} = E(W^2_{mn(N+1)+4}) \tag{3-69}$$

$$\sigma^2_{V_{y_2}} = E(W^2_{mn(N+1)+5})$$

$$\sigma^2_{V_{z_2}} = E(W^2_{mn(N+1)+6})$$

In effect, we examine the effects of inserting a column of ones in the regressor

matrix, H, which is intended to absorb truncation errors caused by linearization of the

RHS of equation (3-26). This also has the effect of allowing the estimation of clock bias

differences, as indicated in Equation (3-49); however, we are mainly concerned with the

estimation of user 1's position and velocity variables.

3.4 Summary

This chapter has described the theory and overall implementation methodology of the developed algorithm. Alternative decentralized estimation algorithms are outlined in Appendix A. Chapter 4 presents the simulation results of, and validates, the algorithm's ability to correctly estimate the parameters of interest.

4 Simulation Results

4.1 Overview

This chapter presents the results of the testing of the novel DGPS algorithm. The estimation of the position and velocity of the mobile users is investigated.

4.2 Simulation Scenarios

Several cases are examined and are summarized in Table 2.

Table 2. Simulation Scenario Summary

Scenario	Reference Accuracy σ (m)	Receiver Noise σ (m)	Time Duration (s)	Number of Measurement Epochs	Number of Satellites, n	Satellite Clock Bias τ_s (m)	Notes
A	0.0001, 0.75, 1.5, 5, 10	0.75, 1.5, 5	2	5	5	100	Prior Reference Position and Velocity Information
B	0.0001, 0.75, 1.5, 5, 10	0.75, 1.5, 5	2	3	5	100	Prior Reference Position and Velocity Information
C	0.0001, 0.75, 1.5, 5, 10	0.75, 1.5, 5	2	3	5	100	Prior Reference Position Information Only
D	0.0001, 0.75, 1.5, 5, 10	0.75, 1.5, 5	10	11	5	100	Prior Reference Position Information Only
E	0.0001, 0.75, 1.5, 5, 10	0.75, 1.5, 5	1	11	5	100	Prior Reference Position Information Only
F	0.0001, 0.75, 1.5, 5, 10	0.75, 1.5, 5	1	11	5	30	Prior Reference Position and Velocity Information
G	0.0001, 0.75, 1.5, 5, 10	0.75, 1.5, 5	2	5	8	100	Prior Reference Position and Velocity Information
H	-	0.75, 1.5, 5	2	5	8	100	No Prior Information
I	0.0001, 0.75, 1.5, 5, 10	0.75, 1.5, 5	1	1	8	100	Prior Reference Position and Velocity Information
J	0.0001	0.75, 1.5, 5	1	1	8	100	Single Difference DGPS

In all the simulation scenarios, two ($m=2$) mobile users traverse parallel tracks, approximately 180 nautical miles above the surface of the earth and separated by 10,000

meters. The users' velocities are 100 meters per second in the x-direction

$(V_{x_1} = 100\, m/s, V_{x_2} = 100\, m/s)$ and zero in the y and z-directions. Both of the users' clock

biases are fixed at five meters $(\tau_k = 5\, meters)$. All satellites are subject to the same clock

bias, viz., $\tau_{s_i} = 100$ meters for $i = 1, 2, \ldots, n$, with the exception of Scenario F.

In the simulation experiment, the actual user 2 initial position is randomly chosen and

is normally distributed about the nominal initial position according to the σ specified in

the table; the latter gauges our confidence in the user 2 positioning prior information.

Both the nominal user 2 initial position and the σ information are provided to the DGPS

estimation algorithm, but not the actual user 2 position used to generate the pseudorange

data given to the algorithm. Finally, the algorithm's performance is gauged by measuring

the distance of the computed position estimate from the actual true position. This applies

to both user 1 and user 2. For each simulation scenario, 100 Monte Carlo runs were

performed. Ten iterations (L=10) for the Iterated Least Squares (ILS) algorithm were

performed for all Scenarios.

4.2.1 Modeling Methodology

The simulation experiment examines the situation of two mobile users moving along

parallel tracks over a specified (short) time interval. The number of satellites in view of

both receivers is held constant at five for Scenarios A-F and eight for Scenarios G-J). A

flow chart of the steps taken during the simulation is depicted in Figure 3.

4-2
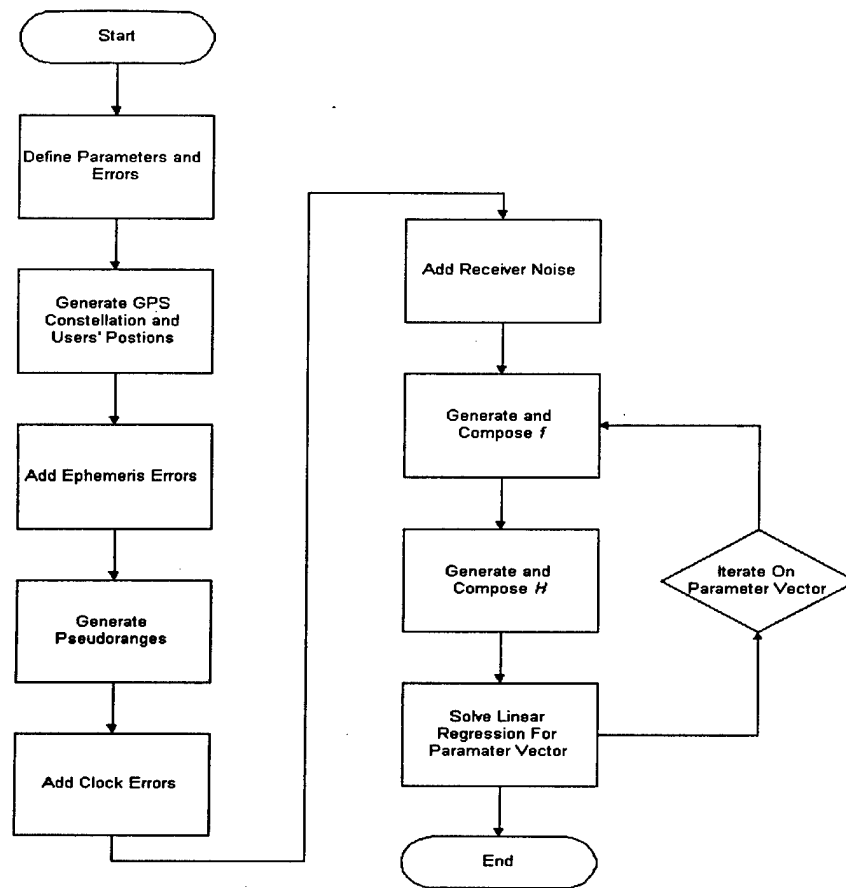
Figure 3.   **Simulation Experiment Flow Chart**

4.2.2 Statistics Examined

Of course, of paramount interest in examination of the data was to determine how well the algorithm was able to estimate the position and velocity of the two receivers. The users' positions were compared to the true (known) positions. The Root Mean Square of these error terms was calculated as

$$r.m.s._{Error} = \sqrt{\frac{\overline{X}_{Error}^2 + \overline{Y}_{Error}^2 + \overline{Z}_{Error}^2}{3}} \qquad (4\text{-}1)$$

where

$$\overline{X}_{Error} = \frac{\sum_{k=1}^{100}(x-\hat{x}_k)}{100}, \quad \overline{Y}_{Error} = \frac{\sum_{k=1}^{100}(y-\hat{y}_k)}{100}, \quad \overline{Z}_{Error} = \frac{\sum_{k=1}^{100}(z-\hat{z}_k)}{100} \qquad (4\text{-}2)$$

The experimental covariance was calculated at the end of the 100 Monte Carlo runs

as

$$\sigma_{exp} = \sqrt{\frac{\sum_{k=1}^{100}\|\hat{x}_k - x\|_2^2}{100}} \qquad (4\text{-}3)$$

Additionally, the predicted covariance was calculated as the average of the predicted

covariance

$$\sigma_{predicted} = \sqrt{\frac{\sum_{k=1}^{100}\left(\sigma_{D_x}^2 + \sigma_{D_y}^2 + \sigma_{D_z}^2\right)}{100}} \qquad (4\text{-}4)$$

Where $\sigma_{D_x}^2, \sigma_{D_y}^2, \sigma_{D_z}^2$ is comprised of the relevant diagonal components of

$(H_1^T R^{-1} H_1)^{-1}$.

4.3   Simulation Results

The data generated from the simulations is documented in Appendix A. The

algorithm's ability to accurately estimate the parameters of interest to the users was

dependent on the accuracy of the reference station's prior information. Uncertainty in the

reference position has a slightly greater impact on the ability of the algorithm to estimate

the users' parameters than the receiver's noise variance.

4.3.1 Effects of Varying Reference Position Accuracy and Receiver Noise

The effect of varying both the uncertainty in the reference position and the receiver noise (utilizing Scenario B's data) on the algorithm's ability to estimate the user's position is illustrated in Figure 4.
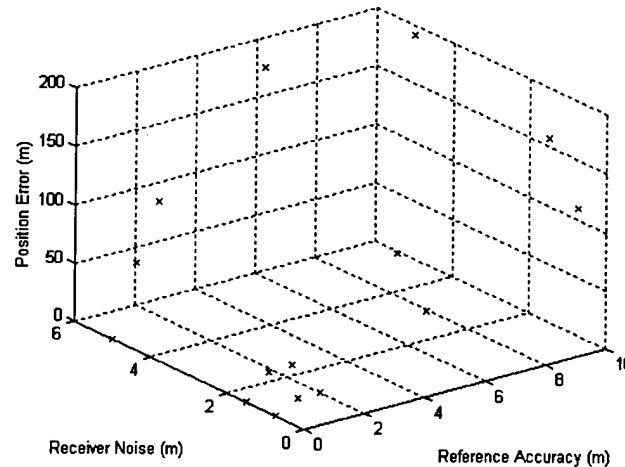
Figure 4. **Position Estimation Error Trend By Varying Parameters**

Similarly, the effect of varying the receiver noise intensity and the reference receiver's positioning accuracy on the users' velocity estimate is shown in Figure 5.
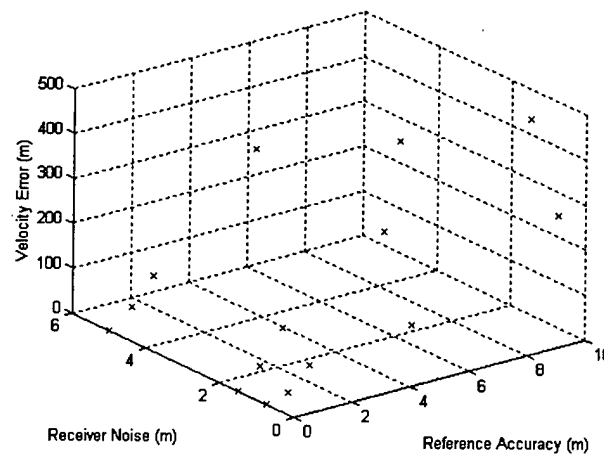
Figure 5. **Velocity Estimation Error Trend By Varying Parameters**

4-5

4.3.2 Results Utilizing Five Satellites

Scenarios A and B entailed prior information on User 2's position and velocity whereas scenarios C-E utilized only User 2's position information. Interestingly, the scenarios without prior velocity information yielded slightly better positions, and approximately equal velocity information for User 1.

The effect of having varying degrees of accuracy in the reference receiver's position and velocity information in Scenarios A-E is further examined in Figures 6 and 7. From Figure 6, with a fixed receiver noise intensity of 1.5 meters, it's obvious that the algorithm's ability to accurately estimate User 1's position deteriorates rapidly as the uncertainty in the reference position increases. In general, after approximately 1 meter of error in the reference position, the algorithm produces large (> 50m), and, possibly unacceptable errors.
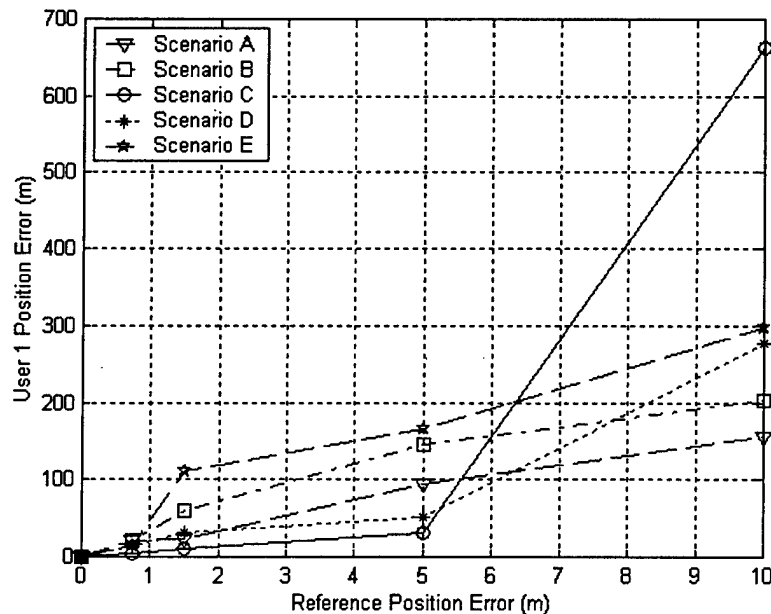
Figure 6.   Effects of Reference Position Error On Position Estimation Error

Similarly, Figure 7 depicts the algorithm's ability to estimate User 1's velocity for

Scenarios A-F with a fixed receiver noise of 1.5 meters. A more linear dependence of the

errors on the reference position accuracy is evident as the accuracy in the reference

position decreases.
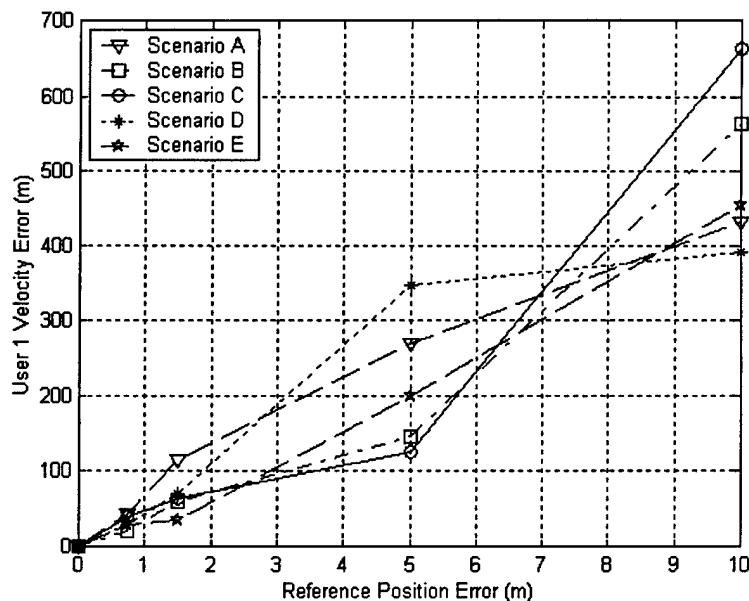
Figure 7.   Effects of Reference Position Error On Velocity Estimation Error

Figures 8 and 9 examine Scenarios A-E when the receiver noise is varied and the

accuracy of the reference station is held to 1.5 meters. The 1.5-meter values used for the

receiver noise and reference position accuracy was chosen because it represents the

average value simulated for the respective noises.

4-7
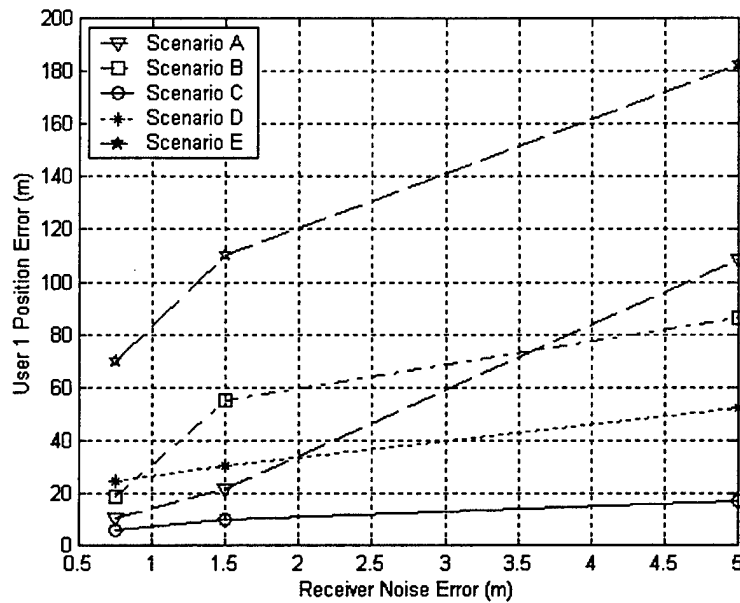
Figure 8. **Effects of Receiver Noise Intensity On Position Estimation Error**
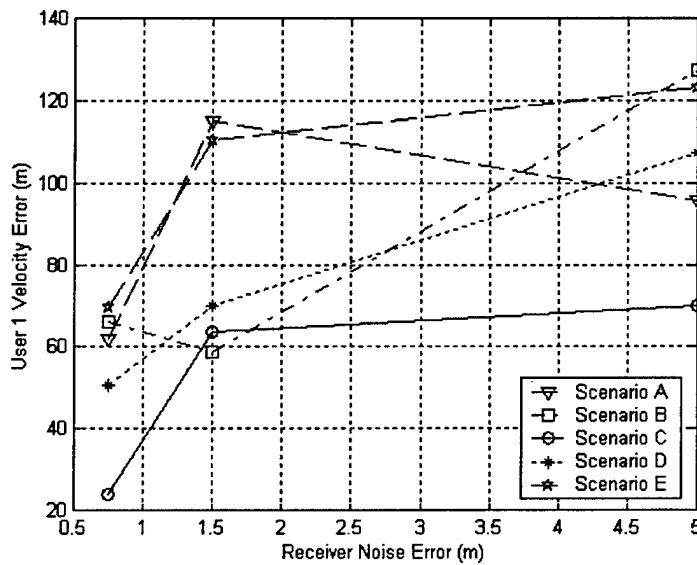
Figure 9. **Effects of Receiver Noise Intensity On Velocity Estimation Error**

As expected, the algorithm provides worse estimates as the receiver noise increases.

While the position accuracy is only slightly better than in the previous case where the

receiver noise is held constant and the reference station accuracy is varied, the velocity

error is slightly worse.

Scenario D was devised to see if not having prior velocity information over a longer observation interval (10 seconds) would have a noticeable detrimental effect. The results (see Table 13 and Table 14) indicate that the algorithm is able to estimate the parameters to a similar degree of accuracy as when using prior velocity information.

A scenario (F), with a smaller degree of range-equivalent satellite clock bias (τ_{sv}), was examined. The data is presented in Table 17 and Table 18. As expected, the overall magnitude of the errors was reduced while following the same trends as indicated in Figures 6-9.

4.3.3 Results Utilizing Eight Satellites

The number of satellites visible to the users was increased from 5 to 8 for Scenarios G-J. The purpose of including these Scenarios was to examine the effect of introducing both more satellites and improved geometry on the algorithm's ability to estimate the parameters of interest. The additional three satellites were chosen from the available constellation to provide the best geometry for solving for the kinematic variables.

Scenarios G and H were simulated with eight satellites ($n=8$) over a time duration of two seconds ($T_s = 2$) and a sample rate of 0.5 seconds (ΔT). As shown in Table 19 and Table 20, the estimates were slightly improved from those obtained in the previous scenarios for Scenario G, while Scenario H displayed the expected results of not incorporating the prior information of the User 2's position and velocity.

4.3.3.1 Single Measurement Epoch

Scenarios I and J examine the effects of conducting a single epoch measurement with

n=8 (eight satellites) and good satellite geometry. As shown in Table 3, the novel

algorithm was able to estimate the position of the users accurately. The realized standard

deviations for the positions show that this was slightly worse solution than that obtained

with more measurement epochs.

Table 3. (I) Users' Position and Sigma Values (N=1, n=8, ΔT=1s, T=1s)

Reference Accuracy (m)	Receiver Noise (m)	User1 Position Error (m)	Predicted User 1 Pos. σ (m)
0.0001	0.75	0.501	1.583
0.0001	1.5	0.875	2.945
0.0001	5	0.841	9.599
0.75	0.75	0.502	2.003
0.75	1.5	1.571	3.165
0.75	5	0.353	9.664
1.5	0.75	0.907	5.151
1.5	1.5	2.944	5.615
1.5	5	1.558	10.550
5	0.75	2.535	10.073
5	1.5	2.913	10.302
5	5	3.930	13.354

Finally, Scenario J was conducted to compare the data obtained from Scenario I with

the estimation performance of a conventional pseudorange differencing-based algorithm

as described in Chapter 2. The results from this simulation indicate that the conventional

algorithm produced comparable results to those produced in Scenario I, provided that the

reference station's (User 2) position is accurately known (σ_{Ref} = 0.0001m).

Table 4. Position Errors For Conventional DGPS (n=8, N=1)

Receiver Noise (m)	User1 Position Error (m)	User1 Clock Error (m)	Predicted User 1 Pos. σ (m)	Exp. User1 Pos. σ (m)	Predicted User 1 Clock σ (m)	Exp. User1 Clock σ (m)
0.75	0.290	-0.534	1.355	0.983	0.688	0.495
1.5	0.117	-0.441	1.355	2.172	0.688	1.048
5	0.528	-0.082	1.355	7.100	0.688	3.508

4.3.4 Analysis of Relative Distance

The estimation of the relative distance between the two users was also examined. The results are presented in Table 5. In all Scenarios, the magnitude of the relative distance error was less than the absolute positioning errors. This indicates that the errors affecting the algorithm's ability to correctly resolve the parameters affects both users.

Table 5. Relative Distance Errors

Reference Accuracy (m)	Receiver Noise (m)	Scenario A	Scenario B	Scenario C	Scenario D	Scenario E	Scenario F	Scenario G	Scenario H
0.0001	0.75	0.374	0.516	0.609	0.607	0.432	0.535	5.739	26.075
0.0001	1.5	0.535	1.010	0.326	0.528	0.627	0.437	16.839	20.763
0.0001	5	0.553	0.544	0.581	0.244	0.337	0.552	61.649	21.676
0.75	0.75	14.524	8.760	0.188	6.343	6.156	11.321	4.044	31.805
0.75	1.5	12.048	16.374	2.034	0.095	15.387	25.930	35.547	31.870
0.75	5	69.900	27.546	4.271	16.757	33.574	92.805	9.327	53.98
1.5	0.75	12.246	12.493	7.632	16.298	37.828	58.785	97.788	183.913
1.5	1.5	26.122	37.696	13.935	19.322	54.151	44.301	206.721	367.860
1.5	5	37.389	36.064	24.483	7.917	34.877	16.246	323.568	622.387
5	0.75	6.308	1.053	47.593	85.898	43.317	122.176	263.563	646.869
5	1.5	45.457	21.143	35.265	81.764	60.051	212.942	221.462	713.341
5	5	5.870	95.507	31.118	60.695	12.014	3.445	168.773	387.616

4.3.5 Analysis of Clock Errors

As seen from Equation (3-52), the new parameter vector $\hat{\theta}_1$ does not strictly attempt to estimate the user and satellite clock values. Instead, a linear combination of clock errors terms is estimated. Since, in the simulation, the users have equal clock biases and the satellites have equal clock biases, the algorithm should produce near zero estimates except for the additive clock error addition where User 2's clock error term is added to the clock bias of satellite 5.

This combination should have the effect of 'collecting' modeling errors introduced into the linear regression by linearization. As can be seen from Table 6 (or graphically in

Figure 10 for Scenario B), the algorithm consistently produces the expected results for

the (τ_1-τ_2) term.

Table 6. Transformed Clock Variables

Reference Accuracy (m)	Receiver Noise (m)	$\tau_1 - \tau_2$ (m)	$\tau_2 + \tau_{s_5}$ (m)	$\tau_{s_1} - \tau_{s_5}$ (m)	$\tau_{s_2} - \tau_{s_5}$ (m)	$\tau_{s_3} - \tau_{s_5}$ (m)	$\tau_{s_4} - \tau_{s_5}$ (m)
0.0001	0.75	-0.034	5.045	-0.011	-0.063	-0.037	-0.028
0.0001	1.5	-0.089	5.070	-0.078	0.015	0.011	0.059
0.0001	5	-0.033	4.862	0.182	0.278	0.129	0.158
0.75	0.75	0.087	17.371	-0.197	-20.227	2.636	-19.911
0.75	1.5	0.178	30.116	-1.080	-45.673	-13.272	-26.159
0.75	5	0.045	7.589	85.913	29.785	-13.884	69.589
1.5	0.75	0.053	20.244	-0.071	-26.232	-2.961	-19.439
1.5	1.5	0.066	-9.871	28.928	40.662	14.369	30.774
1.5	5	-0.010	-131.456	100.679	289.549	79.108	205.322
5	0.75	-0.053	-43.120	75.820	108.145	-21.389	140.537
5	1.5	-0.092	-75.103	148.258	193.167	-20.328	237.859
5	5	-0.256	-131.729	226.813	302.238	-103.528	441.550
10	0.75	-0.082	-14.536	150.171	87.854	-41.653	169.766
10	1.5	0.062	-24.641	224.133	134.501	-50.512	244.681
10	5	0.450	-213.808	307.755	494.541	-17.351	548.593

However, the algorithm only was able to produce the near the desired estimates when

the reference station's position uncertainty and receiver noise were less than 1 meter.
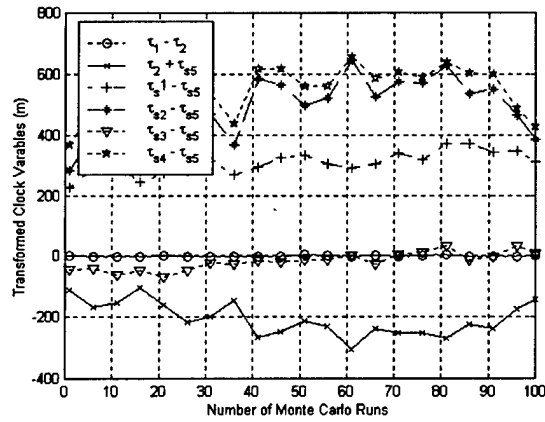
Figure 10.   Clock Performance Trend

4.4 Summary

This chapter presented the performance results of the novel algorithm described in Chapter 3. The algorithm was able to predict the users' positions and velocities within expected levels. It was observed that uncertainty in the reference position had a slightly greater effect on the estimation of the parameters than did variation of the receiver noise intensity. Note, however, that the novel algorithm allows for accounting for the degree of uncertainty in the reference station's position.

A significant change in the algorithms' estimation performance was not evident with an increase in the duration, T, of the observation interval. The performance does slightly improve with the number of satellites visible to the receivers. Additionally, the comparison of the novel algorithm with conventional DGPS techniques over a single measurement epoch yielded similar results. All of the data generated from the simulations are included in Appendix A.

5 Conclusions

5.1 Overview

This thesis presents the theory, modeling methodology and results of a novel DGPS algorithm that estimates mobile users' position and velocity. Also presented are recommendations for future research topics stemming from this research.

5.2 Conclusions

A novel DGPS algorithm was developed to estimate users' positions and velocities utilizing only pseudorange measurements. Simulations were performed to validate the algorithm's ability to estimate the variables of interest.

One of the benefits of using the novel algorithm is its ability to account for the level of uncertainty in the reference receiver's position. As expected, it was shown that the results are very dependent on the accuracy of the reference station's position. When uncertainty in the reference station's position or velocity information was introduced, the algorithm's estimates were correspondingly in error. Also, since the kinematics of the platforms were modeled accurately, there was not a significant error introduced as the duration, T, was increased.

5.3 Recommendations

The following are possible extensions of this research

1. The current algorithm incorporates a simple linear motion model into the algorithm. A more realistic model could be introduced to better represent the motion of a user.

For this example, since the receiver platforms were satellites, a Keplerian model could easily be incorporated.

2. Since carrier phase measurements are inherently more accurate, allowing the algorithm to utilize carrier phase measurements should greatly decrease the errors in estimating both position and velocity of the users.

3. Since the algorithm has the ability to weight measurements, enhance the algorithm to process both pseudorange and carrier phase measurements simultaneously is recommended.

Acronym List

AFIT	Air Force Institute of Technology
AFRL	Air Force Research Laboratory
CPGPS	Carrier Phase Global Positioning System
DCM	Direction Cosine Matrix
ECEF	Earth-Centered, Earth-Fixed
EKF	Extended Kalman Filter
GPS	Global Positioning System
INS	Inertial Navigation System
PR	Pseudorange
RMS	Root-Mean-Square
SA	Selective Availability
SV	Satellite Vehicle
GDOP	Geometric Dilution Of Precision
UERE	User Equivalent Range Error

Appendix A: Simulation Results

Table 7. (A) Position and Velocity Errors (ΔT=0.5s, T=2s)

Reference Accuracy (m)	Receiver Noise (m)	User1 Position Error (m)	User1 Velocity Error (m)	User2 Position Error (m)	User2 Velocity Error (m)
0.0001	0.75	0.121	0.025	0.000	0.000
0.0001	1.5	0.105	0.009	0.000	0.000
0.0001	5	0.170	0.166	0.000	0.000
0.75	0.75	9.522	13.559	0.120	14.074
0.75	1.5	20.635	43.202	0.089	18.381
0.75	5	60.648	40.844	0.065	12.700
1.5	0.75	10.335	62.005	0.145	49.089
1.5	1.5	21.873	114.891	0.139	69.488
1.5	5	108.567	95.764	0.148	75.995
5	0.75	55.732	89.215	0.576	120.701
5	1.5	93.957	268.863	0.580	227.931
5	5	198.026	317.622	0.438	328.642
10	0.75	109.641	247.502	0.851	266.362
10	1.5	156.964	432.401	0.225	348.554
10	5	192.048	249.430	1.415	193.762

Table 8. (A) Predicted and Exp. σ Values (ΔT=0.5s, T=2s)

Reference Accuracy (m)	Receiver Noise (m)	Predicted User 1 Pos. σ (m)	Predicted User 1 Vel. σ (m)	Predicted User 2 Pos. σ (m)	Predicted User 2 Vel. σ (m)	Exp. User1 Pos. σ (m)	Exp. User1 Vel. σ (m)	Exp. User2 Pos. σ (m)	Exp. User2 Vel. σ (m)
0.0001	0.75	0.966	0.301	0.000	0.000	0.973	0.280	0.000	0.000
0.0001	1.5	1.932	0.602	0.000	0.000	1.905	0.616	0.000	0.000
0.0001	5	6.441	2.006	0.000	0.000	6.507	1.996	0.000	0.000
0.75	0.75	1.328	0.301	0.750	0.265	6.066	0.300	0.780	8.258
0.75	1.5	2.233	0.602	0.750	0.422	10.347	0.615	0.802	12.973
0.75	5	6.613	2.006	0.750	0.655	13.505	1.939	0.757	2.299
1.5	0.75	1.871	0.301	1.500	0.290	8.178	0.280	1.500	12.051
1.5	1.5	2.657	0.602	1.500	0.530	12.815	0.635	1.503	25.298
1.5	5	6.943	2.006	1.500	1.070	17.762	2.113	1.421	8.313
5	0.75	5.124	0.301	5.000	0.300	22.371	0.309	4.999	47.886
5	1.5	5.481	0.602	5.000	0.594	24.213	0.593	5.156	93.017
5	5	8.855	2.006	5.000	1.768	33.512	2.014	4.907	55.791
10	0.75	10.061	0.301	10.000	0.301	75.271	0.329	10.363	81.878
10	1.5	10.249	0.602	10.000	0.600	46.201	0.597	9.986	129.583
10	5	12.473	2.006	10.000	1.935	53.081	2.038	10.111	175.158

Table 9. (B) Position and Velocity Errors (ΔT=1s, T=2s)

Reference Accuracy (m)	Receiver Noise (m)	User1 Position Error (m)	User1 Velocity Error (m)	User2 Position Error (m)	User2 Velocity Error (m)
0.0001	0.75	0.027	0.080	0.000	0.000
0.0001	1.5	0.331	0.101	0.000	0.000
0.0001	5	0.701	0.535	0.000	0.000
0.75	0.75	8.889	23.364	0.075	13.941
0.75	1.5	18.210	20.492	0.035	12.501
0.75	5	30.832	45.821	0.107	2.884
1.5	0.75	18.921	66.097	0.186	48.909
1.5	1.5	54.970	58.708	0.103	43.047
1.5	5	86.100	127.494	0.228	29.541
5	0.75	24.637	163.388	0.529	219.899
5	1.5	34.682	146.088	0.977	136.687
5	5	79.711	294.304	0.544	163.460
10	0.75	42.061	505.847	0.556	301.496
10	1.5	23.423	564.642	0.953	544.950
10	5	242.424	1033.223	0.443	647.628

Table 10. (B) Predicted and Exp. σ Values (ΔT=1s, T=2s)

Reference Accuracy (m)	Receiver Noise (m)	Predicted User 1 Pos. σ (m)	Predicted User 1 Vel. σ (m)	Predicted User 2 Pos. σ (m)	Predicted User 2 Vel. σ (m)	Exp. User1 Pos. σ (m)	Exp. User1 Vel. σ (m)	Exp. User2 Pos. σ (m)	Exp. User2 Vel. σ (m)
0.0001	0.75	1.188	0.673	0.000	0.000	1.197	0.671	0.000	0.000
0.0001	1.5	2.376	1.346	0.000	0.000	2.427	1.288	0.000	0.000
0.0001	5	7.921	4.486	0.000	0.000	8.175	4.565	0.000	0.000
0.75	0.75	1.470	0.673	0.750	0.447	8.580	0.753	0.792	10.126
0.75	1.5	2.557	1.346	0.750	0.592	6.039	1.326	0.805	3.365
0.75	5	7.988	4.486	0.750	0.725	12.434	4.094	0.730	0.930
1.5	0.75	1.991	0.673	1.500	0.578	8.041	0.637	1.502	15.009
1.5	1.5	2.939	1.346	1.500	0.895	13.025	1.476	1.590	13.385
1.5	5	8.167	4.486	1.500	1.339	23.515	4.440	1.446	10.448
5	0.75	5.176	0.673	5.000	0.662	19.831	0.688	4.811	68.235
5	1.5	5.664	1.346	5.000	1.264	15.372	1.355	4.822	62.518
5	5	9.798	4.486	5.000	2.983	45.660	4.741	5.074	49.168
10	0.75	10.088	0.673	10.000	0.670	36.829	0.721	10.083	100.141
10	1.5	10.353	1.346	10.000	1.323	41.490	1.416	10.148	161.906
10	5	13.276	4.486	10.000	3.853	92.129	4.922	10.157	171.172

Table 11. (C) Position and Velocity Errors ($\Delta T=1s$, $T=2s$, w/o Prior Vel. Data)

Reference Accuracy (m)	Receiver Noise (m)	User1 Position Error (m)	User1 Velocity Error (m)	User2 Position Error (m)	User2 Velocity Error (m)
0.0001	0.75	0.069	0.032	0.000	0.024
0.0001	1.5	0.112	0.081	0.000	0.062
0.0001	5	0.409	0.497	0.000	0.438
0.75	0.75	1.946	13.257	0.095	2.644
0.75	1.5	3.665	38.353	0.126	24.411
0.75	5	5.199	42.187	0.096	43.532
1.5	0.75	5.954	23.962	0.101	44.117
1.5	1.5	9.692	63.595	0.198	50.150
1.5	5	16.936	70.103	0.134	101.472
5	0.75	28.236	98.068	0.899	125.594
5	1.5	30.856	124.313	0.889	193.204
5	5	48.970	143.292	0.491	207.080
10	0.75	86.177	362.613	2.222	389.846
10	1.5	141.344	662.599	0.667	500.345
10	5	147.069	799.588	1.152	777.950

Table 12. (C) Predicted and Exp. σ Values ($\Delta T=1s$, $T=2s$, w/o Prior Vel. Data)

Reference Accuracy (m)	Receiver Noise (m)	Predicted User 1 Pos. σ (m)	Predicted User 1 Vel. σ (m)	Predicted User 2 Pos. σ (m)	Predicted User 2 Vel. σ (m)	Exp. User1 Pos. σ (m)	Exp. User1 Vel. σ (m)	Exp. User2 Pos. σ (m)	Exp. User2 Vel. σ (m)
0.0001	0.75	1.359	0.673	0.000	0.673	1.277	0.635	0.000	0.643
0.0001	1.5	2.718	1.346	0.000	1.346	2.705	1.399	0.000	1.339
0.0001	5	9.060	4.486	0.000	4.485	8.923	4.530	0.000	4.455
0.75	0.75	1.550	0.673	0.750	0.673	2.982	0.651	0.689	7.847
0.75	1.5	2.818	1.346	0.750	1.346	4.287	1.386	0.783	15.431
0.75	5	9.091	4.486	0.750	4.485	9.024	4.703	0.707	9.308
1.5	0.75	2.020	0.673	1.500	0.673	5.532	0.685	1.670	19.904
1.5	1.5	3.100	1.346	1.500	1.346	5.635	1.308	1.511	22.356
1.5	5	9.182	4.486	1.500	4.485	10.572	4.412	1.569	18.775
5	0.75	5.178	0.673	5.000	0.673	16.913	0.745	4.954	71.532
5	1.5	5.682	1.346	5.000	1.346	19.542	1.266	4.911	66.586
5	5	10.334	4.486	5.000	4.485	21.351	4.195	4.845	52.430
10	0.75	10.088	0.673	10.000	0.673	40.394	0.669	9.813	102.063
10	1.5	10.356	1.346	10.000	1.346	45.037	1.368	11.068	176.748
10	5	13.467	4.486	10.000	4.485	37.847	4.099	10.013	123.594

Table 13. (D) Position and Velocity Errors (ΔT=1s, T=10s, w/o Prior Vel. Data)

Reference Accuracy (m)	Receiver Noise (m)	User1 Position Error (m)	User1 Velocity Error (m)	User2 Position Error (m)	User2 Velocity Error (m)
0.0001	0.75	0.089	0.007	0.000	0.011
0.0001	1.5	0.076	0.004	0.000	0.005
0.0001	5	0.387	0.088	0.000	0.029
0.75	0.75	10.623	44.466	0.051	24.835
0.75	1.5	15.068	29.197	0.096	35.867
0.75	5	24.457	40.134	0.090	33.518
1.5	0.75	24.686	50.680	0.082	36.750
1.5	1.5	30.545	70.146	0.063	44.069
1.5	5	52.454	107.299	0.142	90.908
5	0.75	74.645	351.477	0.444	198.974
5	1.5	50.587	347.772	0.370	354.519
5	5	88.012	331.813	0.849	331.081
10	0.75	138.213	490.363	0.533	319.184
10	1.5	278.136	391.972	1.216	510.012
10	5	249.348	346.496	0.315	320.268

Table 14. (D) Predicted and Exp. σ Values (ΔT=1s, T=10s, w/o Prior Vel. Data)

Reference Accuracy (m)	Receiver Noise (m)	Predicted User 1 Pos. σ (m)	Predicted User 1 Vel. σ (m)	Predicted User 2 Pos. σ (m)	Predicted User 2 Vel. σ (m)	Exp. User1 Pos. σ (m)	Exp. User1 Vel. σ (m)	Exp. User2 Pos. σ (m)	Exp. User2 Vel. σ (m)
0.0001	0.75	0.815	0.091	0.000	0.091	0.825	0.095	0.000	0.089
0.0001	1.5	1.630	0.181	0.000	0.181	1.652	0.187	0.000	0.184
0.0001	5	5.434	0.605	0.000	0.604	5.389	0.651	0.000	0.601
0.75	0.75	1.106	0.091	0.750	0.091	7.259	0.077	0.780	16.176
0.75	1.5	1.793	0.181	0.750	0.181	4.523	0.184	0.741	11.605
0.75	5	5.486	0.605	0.750	0.604	9.055	0.638	0.751	8.253
1.5	0.75	1.706	0.091	1.500	0.091	11.992	0.095	1.469	17.979
1.5	1.5	2.213	0.181	1.500	0.181	14.058	0.184	1.466	18.235
1.5	5	5.636	0.605	1.500	0.604	19.791	0.555	1.569	25.370
5	0.75	5.064	0.091	5.000	0.091	57.225	0.089	5.275	120.993
5	1.5	5.256	0.181	5.000	0.181	62.337	0.179	5.175	69.288
5	5	7.376	0.605	5.000	0.604	35.900	0.559	4.815	47.352
10	0.75	10.030	0.091	9.999	0.091	112.815	0.100	10.477	252.383
10	1.5	10.129	0.181	10.000	0.181	77.728	0.190	10.336	109.298
10	5	11.371	0.605	10.000	0.604	92.155	0.609	9.761	86.017

Table 15. (E) Position and Velocity Errors (ΔT=0.1s, T=1s, w/o Prior Vel. Data)

Reference Accuracy (m)	Receiver Noise (m)	User1 Position Error (m)	User1 Velocity Error (m)	User2 Position Error (m)	User2 Velocity Error (m)
0.0001	0.75	0.074	0.003	0.000	0.008
0.0001	1.5	0.102	0.007	0.000	0.022
0.0001	5	0.136	0.083	0.000	0.034
0.75	0.75	4.204	16.381	0.064	8.288
0.75	1.5	13.947	28.286	0.048	20.766
0.75	5	26.981	24.399	0.034	20.005
1.5	0.75	69.744	26.760	0.280	34.320
1.5	1.5	110.278	34.385	0.179	15.596
1.5	5	123.048	48.960	0.274	52.765
5	0.75	182.231	153.778	0.151	73.967
5	1.5	165.995	198.152	0.738	178.045
5	5	150.214	357.960	0.704	322.350
10	0.75	254.858	335.030	1.237	332.509
10	1.5	296.913	455.474	1.187	337.648
10	5	299.469	656.191	1.351	536.431

Table 16. (E) Predicted and Exp. σ Values (ΔT=0.1s, T=1s, w/o Prior Vel. Data)

Reference Accuracy (m)	Receiver Noise (m)	Predicted User 1 Pos. σ (m)	Predicted User 1 Vel. σ (m)	Predicted User 2 Pos. σ (m)	Predicted User 2 Vel. σ (m)	Exp. User1 Pos. σ (m)	Exp. User1 Vel. σ (m)	Exp. User2 Pos. σ (m)	Exp. User2 Vel. σ (m)
0.0001	0.75	0.815	0.091	0.000	0.091	0.826	0.093	0.000	0.095
0.0001	1.5	1.631	0.181	0.000	0.181	1.686	0.184	0.000	0.186
0.0001	5	5.435	0.605	0.000	0.605	5.365	0.605	0.000	0.594
0.75	0.75	1.107	0.091	0.750	0.091	4.719	0.080	0.737	7.984
0.75	1.5	1.794	0.181	0.750	0.181	5.490	0.178	0.696	5.377
0.75	5	5.486	0.605	0.750	0.605	10.855	0.532	0.742	9.227
1.5	0.75	1.706	0.091	1.500	0.091	18.695	0.092	1.553	13.377
1.5	1.5	2.213	0.181	1.500	0.181	12.772	0.192	1.421	16.726
1.5	5	5.637	0.605	1.500	0.605	19.710	0.592	1.452	14.975
5	0.75	5.064	0.091	5.000	0.091	36.894	0.094	5.298	63.592
5	1.5	5.256	0.181	5.000	0.181	44.354	0.212	5.213	45.504
5	5	7.377	0.605	5.000	0.605	58.610	0.599	4.753	75.267
10	0.75	10.031	0.091	10.000	0.091	92.336	0.082	10.090	94.315
10	1.5	10.129	0.181	10.000	0.181	57.472	0.164	10.140	162.576
10	5	11.371	0.605	10.000	0.605	92.283	0.562	10.579	92.118

Table 17. (F) Position and Velocity Errors ($\Delta T=0.1s$, $T=1s$, $\tau_{SV}=30m$)

Reference Accuracy (m)	Receiver Noise (m)	User1 Position Error (m)	User1 Velocity Error (m)	User2 Position Error (m)	User2 Velocity Error (m)
0.0001	0.75	0.057	0.008	0.000	0.000
0.0001	1.5	0.082	0.012	0.000	0.000
0.0001	5	0.098	0.036	0.000	0.000
0.75	0.75	11.934	27.236	0.071	15.323
0.75	1.5	40.327	37.830	0.030	28.444
0.75	5	127.203	46.973	0.075	29.089
1.5	0.75	64.656	61.068	0.054	55.207
1.5	1.5	57.417	143.444	0.178	97.838
1.5	5	77.496	160.669	0.125	142.050
5	0.75	151.865	234.798	0.899	189.707
5	1.5	238.569	336.639	0.514	298.967
5	5	221.235	501.094	1.122	409.442
10	0.75	160.973	562.276	0.778	485.530
10	1.5	282.283	831.210	0.795	657.617
10	5	154.141	1313.504	0.736	1054.391

Table 18. (F) Predicted and Exp. σ Values ($\Delta T=0.1s$, $T=1s$, $\tau_{SV}=30m$)

Reference Accuracy (m)	Receiver Noise (m)	Predicted User 1 Pos. σ (m)	Predicted User 1 Vel. σ (m)	Predicted User 2 Pos. σ (m)	Predicted User 2 Vel. σ (m)	Exp. User1 Pos. σ (m)	Exp. User1 Vel. σ (m)	Exp User2 Pos. σ (m)	Exp. User2 Vel. σ (m)
0.0001	0.75	0.681	0.091	0.000	0.000	0.643	0.091	0.000	0.000
0.0001	1.5	1.362	0.181	0.000	0.000	1.385	0.207	0.000	0.000
0.0001	5	4.541	0.605	0.000	0.000	4.292	0.598	0.000	0.000
0.75	0.75	1.104	0.091	0.750	0.090	9.248	0.102	0.789	12.292
0.75	1.5	1.772	0.181	0.750	0.172	7.059	0.192	0.769	8.291
0.75	5	5.058	0.605	0.750	0.423	17.741	0.584	0.730	8.406
1.5	0.75	1.705	0.091	1.500	0.090	13.163	0.089	1.441	21.929
1.5	1.5	2.208	0.181	1.500	0.179	14.625	0.174	1.499	22.742
1.5	5	5.458	0.605	1.500	0.533	22.757	0.603	1.547	14.341
5	0.75	5.064	0.091	5.000	0.091	44.698	0.084	5.256	48.377
5	1.5	5.256	0.181	5.000	0.181	44.327	0.173	4.791	79.700
5	5	7.361	0.605	5.000	0.597	55.483	0.546	4.824	55.813
10	0.75	10.031	0.091	10.000	0.091	107.375	0.079	9.819	131.843
10	1.5	10.129	0.181	10.000	0.181	74.259	0.181	10.018	98.750
10	5	11.369	0.605	10.000	0.603	65.062	0.612	10.495	146.767

Table 19. (G) Position and Velocity Errors (n=8, ΔT=0.5s, T=2s)

Reference Accuracy (m)	Receiver Noise (m)	User1 Position Error (m)	User1 Velocity Error (m)	User2 Position Error (m)	User2 Velocity Error (m)
0.0001	0.75	3.744	14.164	0.052	13.701
0.0001	1.5	10.105	34.275	0.112	19.913
0.0001	5	76.074	49.446	0.067	17.414
0.75	0.75	14.082	72.221	0.155	70.574
0.75	1.5	26.532	74.746	0.253	26.483
0.75	5	28.400	83.872	0.029	36.528
1.5	0.75	60.803	240.029	0.719	110.769
1.5	1.5	144.471	288.930	0.227	261.866
1.5	5	193.363	303.263	0.256	286.149
5	0.75	177.225	400.646	1.829	273.685
5	1.5	206.973	367.725	1.153	452.736
5	5	286.712	586.073	1.358	468.085
10	0.75	3.744	14.164	0.052	13.701
10	1.5	10.105	34.275	0.112	19.913
10	5	76.074	49.446	0.067	17.414

Table 20. (G) Predicted and Exp. σ Values (n=8, ΔT=0.5s, T=2s)

Reference Accuracy (m)	Receiver Noise (m)	Predicted User 1 Pos. σ (m)	Predicted User 1Vel. σ (m)	Predicted User 2 Pos. σ (m)	Predicted User 2 Vel. σ (m)	Exp. User1 Pos. σ (m)	Exp. User1 Vel. σ (m)	Exp User2 Pos. σ (m)	Exp. User2 Vel. σ (m)
0.0001	0.75	1.074	0.179	0.750	0.173	3.957	0.190	0.756	6.795
0.0001	1.5	1.729	0.359	0.750	0.316	7.531	0.364	0.791	8.234
0.0001	5	5.049	1.195	0.750	0.610	14.709	1.206	0.700	3.163
0.75	0.75	1.676	0.179	1.500	0.178	8.644	0.187	1.461	15.743
0.75	1.5	2.149	0.359	1.500	0.346	12.177	0.384	1.452	41.047
0.75	5	5.346	1.195	1.500	0.897	15.003	1.128	1.387	12.334
1.5	0.75	5.053	0.179	5.000	0.179	34.865	0.160	5.065	78.510
1.5	1.5	5.213	0.359	5.000	0.357	37.922	0.332	4.711	102.651
1.5	5	7.162	1.195	5.000	1.153	32.173	1.218	5.186	80.231
5	0.75	10.025	0.179	10.000	0.179	43.973	0.180	10.134	104.954
5	1.5	10.105	0.359	10.000	0.358	65.897	0.328	10.697	101.361
5	5	11.173	1.195	10.000	1.184	94.376	1.288	10.632	124.427
10	0.75	1.074	0.179	0.750	0.173	3.957	0.190	0.756	6.795
10	1.5	1.729	0.359	0.750	0.316	7.531	0.364	0.791	8.234
10	5	5.049	1.195	0.750	0.610	14.709	1.206	0.700	3.163

Table 21. (H) Position and Velocity Errors (n=8, ΔT=0.5s, T=2s)

Reference Accuracy (m)	Receiver Noise (m)	User1 Position Error (m)	User2 Position Error (m)
0.0001	0.75	0.285	0.000
0.0001	1.5	0.225	0.000
0.0001	5	0.255	0.000
0.75	0.75	4.600	0.056
0.75	1.5	22.792	0.055
0.75	5	99.354	0.116
1.5	0.75	9.679	0.122
1.5	1.5	30.173	0.231
1.5	5	138.666	0.125
5	0.75	36.017	0.229
5	1.5	89.793	0.418
5	5	106.543	0.506
10	0.75	27.168	0.925
10	1.5	85.704	1.035
10	5	17.576	1.483

Table 22. Predicted and Exp. σ Values (n=8, ΔT=0.5s, T=2s)

Reference Accuracy (m)	Receiver Noise (m)	Predicted User 1 Pos. σ (m)	Predicted User 2 Pos. σ (m)	Exp. User1 Pos. σ (m)	Exp User2 Pos. σ (m)
0.0001	0.75	3.486	1.732	0.714	0.000
0.0001	1.5	1.743	1.732	1.508	0.000
0.0001	5	0.523	1.732	5.129	0.000
0.75	0.75	1.745	0.002	3.071	0.732
0.75	1.5	1.222	0.002	7.738	0.758
0.75	5	0.475	0.002	18.152	0.755
1.5	0.75	1.047	0.001	8.753	1.472
1.5	1.5	0.873	0.001	10.417	1.457
1.5	5	0.422	0.001	25.375	1.540
5	0.75	0.342	0.001	44.340	5.153
5	1.5	0.333	0.001	28.225	5.033
5	5	0.262	0.001	35.210	5.053
10	0.75	0.173	0.001	61.491	9.071
10	1.5	0.172	0.001	44.584	9.752
10	5	0.157	0.001	74.473	9.820

Table 23. Position and Velocity Errors (n=8, ΔT=0.5s, T=2s, , w/o Prior Vel. Info.)

Receiver Noise (m)	User1 Position Error (m)	User1 Velocity Error (m)	User2 Position Error (m)	User2 Velocity Error (m)
0.75	659.091	0.027	659.014	0.025
1.5	600.793	0.048	600.872	0.102
5	3809.023	0.227	3809.468	0.171

Table 24. Position and Velocity Errors (n=8, ΔT=0.5s, T=2s, w/o Prior Vel. Info.)

Receiver Noise (m)	Predicted User 1 Pos. σ (m)	Predicted User 1Vel. σ (m)	Predicted User 2 Pos. σ (m)	Predicted User 2 Vel. σ (m)	Exp. User1 Pos. σ (m)	Exp. User1 Vel. σ (m)	Exp User2 Pos. σ (m)	Exp. User2 Vel. σ (m)
0.75	2978.031	0.158	2978.699	0.158	2933.082	0.160	2933.770	0.160
1.5	5912.051	0.317	5913.399	0.317	5887.641	0.303	5888.969	0.332
5	19535.204	1.058	19539.733	1.058	18600.126	1.036	18604.904	1.051

Appendix B: Decentralized Approaches

Measurement noise effects mitigation in GPS/DGPS – Indirect approach

Assume that at the conclusion of the ILS iteration sequence, the vehicle's position vector satisfies

$$x = N(\hat{x}, P) \qquad \text{(B-1)}$$

where

$$P = \sigma^2 I_3 \qquad \text{(B-2)}$$

Here, the position equation can be considered as

$$\hat{x} = x + v \qquad \text{(B-3)}$$

where

$$E(vv^T) = P = \sigma^2 I_3 \qquad \text{(B-4)}$$

While standard DGPS techniques obtain a precise estimate of position, the receiver measurement noise is increased (see Table 1). Rather than fight the ill effects of measurement noise at the reference station algorithm level, a centralized and therefore theoretically more rigorous (and better) algorithm is developed. Specifically, one stipulates the following behavioral assumption concerning the vehicle's dynamics

$$x(t) = x_0 + vt + \frac{1}{2}at^2 \qquad \text{(B-5)}$$

where the three (unknown) vectors $x_0, v, a \in \Re^n, (n = 9)$. A temporal horizon, T, is chosen such that $0 \leq t \leq T$. Therefore, the parameter vector is

$$\theta = \begin{pmatrix} x_\theta \\ v \\ a \end{pmatrix} \in R^9 \qquad \text{(B-6)}$$

A sampling interval, ΔT, is also chosen which allows defining the number of samples as

$$N = \frac{T}{\Delta T} \qquad \text{(B-7)}$$

The choice of T and ΔT is determined by the dynamics and maneuverability of the vehicle under consideration. Also for estimation purposes, it is desirable to have

$$N \geq 2n^2 \qquad \text{(B-8)}$$

The available GPS measurements are of the form

$$Z_i = \hat{x}(i\Delta T), \; i = 0,1,...,N \qquad \text{(B-9)}$$

A moving data window will be used to solve the least squares problem in the vector parameter of interest, θ, i.e.

$$\min_\theta \sum_{i=0}^{N} \| x(i\Delta T) - Z_i \|_2^2 \qquad \text{(B-10)}$$

Now, Equation (B-5) is written as

$$x(i\Delta T) = x_\theta + v \cdot (i\Delta T) + a\frac{1}{2}(i\Delta T^2)$$

$$= [I_3 \vdots i\Delta \quad _3 \vdots \frac{1}{2}(i\Delta \quad ^2 I_3] \theta \qquad \text{(B-11)}$$

Defining the matrix

$$M_{i_{3x9}} = [I_3 \vdots (i\Delta T)I_3 \vdots \frac{1}{2}(i\Delta T)^2 I_3] \qquad \text{(B-12)}$$

allows Equation (B-11) to be re-written as

$$x(i\Delta T) = M_i\theta \tag{B-13}$$

Using the new notation, the cost function to be minimized becomes

$$J = \sum_{i=0}^{N} \left\| x(i\Delta T) - Z_i \right\|_2^2 = \sum_{i=0}^{N} (M_i\theta - Z_i)^T(M_i\theta - Z_i) \tag{B-14}$$

Since the cost function is quadratic, setting the derivative to zero, i.e., can minimize it.

$$\frac{dJ}{d\theta} = 0 \tag{B-15}$$

which yields

$$\sum_{i=0}^{N} M_i^T(M_i\theta - Z_i) = 0$$

$$\Rightarrow (\sum_{i=0}^{N} M_i^T M_i)\theta = \sum_{i=0}^{N} M_i^T Z_i \tag{B-16}$$

Solving for the parameter vector of interest as

$$\hat{\theta} = (\sum_{i=0}^{N} M_i^T M_i)^{-1} \sum_{i=0}^{N} M_i^T Z_i \tag{B-17}$$

Now,

$$M_i^T M_i = \begin{bmatrix} I_3 & (i\Delta T)I_3 & \frac{1}{2}(i\Delta T)^2 I_3 \\ (i\Delta T)I_3 & (i\Delta T)^2 I_3 & \frac{1}{2}(i\Delta T)^3 I_3 \\ \frac{1}{2}(i\Delta T)^2 I_3 & \frac{1}{2}(i\Delta T)^3 I_3 & \frac{1}{4}(i\Delta T)^4 I_3 \end{bmatrix} \tag{B-18}$$

To allow further simplification of the notation, define

$$M = \sum_{i=0}^{N} M_i^T M_i \tag{B-19}$$

Therefore,

$$\sum_{i=0}^{N} M_i^T Z_i = \begin{bmatrix} \sum_{i=0}^{N} \hat{x}(i\Delta \\ \Delta \sum_{i=0}^{N} \hat{x}(i\Delta \\ \frac{1}{2}\Delta^{\,2} \sum_{i=0}^{N} \hat{x}(i\Delta \end{bmatrix}$$

(B-20)

Simpler Notation

If the vehicle dynamics are rather benign, the vehicle's position, Equation (B-5) can be simplified by removing the acceleration term. This will result in a less accurate solution, but simplifies required computations. The simplified position equation can be written as

$$x(i\Delta T) = x_0 + v \cdot (i\Delta T)$$

(B-21)

with a parameter vector consisting of the variables of interest

$$\theta = \begin{pmatrix} x_0 \\ v\Delta T \end{pmatrix} \in \Re^6$$

(B-22)

Now, the cost function can be similarly developed, as in Equation (B-14), and defined as

$$J = \sum_{i=0}^{N} (x_0 + vi\Delta T - Z_i)^T (x_0 + vi\Delta T - Z_i)$$

$$= \sum x_0^T x_0 + (\Delta T)^2 i^2 v^T v + Z_i^T Z_i + 2x_0^T v\Delta Ti - 2x_0^T Z_i - 2\Delta Ti v^T Z_i$$

(B-23)

The minimization of Equation (B-23)

$$\min_{\theta} \sum_{i=0}^{N} \left[x_0^T x_0 + (v\Delta T)^T (v\Delta T) + 2i x_0^T (v\Delta T) - 2x_0^T Z_i - 2Z_i^T (v\Delta T)i \right]$$

(B-24)

yields

$$\Rightarrow \begin{cases} \sum_{i=0}^{N} x_0 + i(v\Delta T) = \sum_{i=0}^{N} Z_i \\ \sum_{i=0}^{N} ix_0 + i^2(v\Delta T) = \sum_{i=0}^{N} iZ_i \end{cases} \tag{B-25}$$

This allows for solving of the vector θ by

$$\begin{bmatrix} N+1 & \frac{1}{2}N(N+1) \\ \frac{1}{2}N(N+1) & \frac{1}{6}N(N+1)(2N+1) \end{bmatrix} \theta = \begin{bmatrix} \sum_{i=0}^{N} Z_i \\ \sum_{i=0}^{N} iZ_i \end{bmatrix} \tag{B-26}$$

or, after re-arranging terms,

$$\begin{bmatrix} 1 & \frac{1}{2}N \\ \frac{1}{2}N & \frac{1}{6}N(2N+1) \end{bmatrix} \theta = \frac{1}{N+1}\begin{bmatrix} \sum_{i=0}^{N} Z_i \\ \sum_{i=0}^{N} iZ_i \end{bmatrix} \tag{B-27}$$

Now, solving for θ yields

$$\hat{\theta} = \frac{12}{N(N+2)}\begin{bmatrix} \frac{1}{6}N(2N+1) & -\frac{1}{2}N \\ -\frac{1}{2}N & 1 \end{bmatrix}\cdot\frac{1}{N+1}\begin{bmatrix} \sum_{i=0}^{N} Z_i \\ \sum_{i=0}^{N} iZ_i \end{bmatrix} \tag{B-28}$$

permits explicitly expressing the variables of interest as

$$\hat{x}_0 = \frac{2(2N+1)}{(N+1)(N+2)}\sum_{i=0}^{N} Z_i - \frac{6}{(N+1)(N+2)}\sum_{i=0}^{N} iZ_i \tag{B-29}$$

and,

$$\Delta T\hat{v} = -\frac{6}{(N+1)(N+2)}\sum_{i=0}^{N} Z_i + \frac{12}{N(N+1)(N+2)}\sum_{i=0}^{N} iZ_i \tag{B-30}$$

Examples

For the situation where N=1 and using Equations (B-29) and (B-30) yield

$$\hat{x}_0 = \hat{x}(0)$$

$$\hat{v} = \frac{1}{\Delta T}[\hat{x}(1) - \hat{x}(0)] \qquad \text{(B-31)}$$

as expected. For the case N = 2,

$$\hat{x}_0 = \frac{1}{6}[5\hat{x}(0) + 2\hat{x}(1) - \hat{x}(2)]$$

$$\hat{v} = \frac{1}{2\Delta T}[\hat{x}(2) - \hat{x}(0)] \qquad \text{(B-32)}$$

and, similarly, for the case when N=3,

$$\hat{x}_0 = \frac{1}{10}[7\hat{x}(0) + 4\hat{x}(1) + \hat{x}(2) - 2\hat{x}(3)]$$

$$\hat{v} = \frac{1}{10\Delta T}[-3\hat{x}(0) - \hat{x}(1) + \hat{x}(2) + 3\hat{x}(3)] \qquad \text{(B-33)}$$

Of course, solving for cases where N > 1 require the knowledge of previous values,

i.e. for the case of N=3 would require knowledge of

$$\hat{x}(0), \hat{x}(1), \hat{x}(2), and \; \hat{x}(3) \qquad \text{(B-34)}$$

The notation can be improved to allow easier reading. For the case of N=3, let

$$\hat{\hat{x}}(0) = \frac{1}{10}[7\hat{x}(0) + 4\hat{x}(1) + \hat{x}(2) - 2\hat{x}(3)] \qquad \text{(B-35)}$$

and

$$\hat{\hat{x}}(1) = \hat{\hat{x}}(0) + \hat{v}\Delta T$$

$$= \frac{1}{10}[7\hat{x}(0) + 4\hat{x}(1) + \hat{x}(2) - 2\hat{x}(3)] + \frac{1}{10}[-3\hat{x}(0) - \hat{x}(1) + \hat{x}(2) + 3\hat{x}(3)] \qquad \text{(B-36)}$$

$$= \frac{1}{10}[4\hat{x}(0) + 3\hat{x}(1) + 2\hat{x}(2) + \hat{x}(3)]$$

Actually, we are interested in the (improved) estimate of the state at time 3, $\hat{\hat{x}}(3)$, now

$$
\begin{aligned}
\hat{\hat{x}}(3) &= \hat{\hat{x}}(0) + 3(\hat{v}\Delta T) \\
&= \frac{1}{10}[7\hat{x}(0) + 4\hat{x}(1) + \hat{x}(2) - 2\hat{x}(3) - 9\hat{x}(0) - 3\hat{x}(1) + 3\hat{x}(2) + 9\hat{x}(3)]
\end{aligned}
\tag{B-37}
$$

which gives,

$$
\hat{\hat{x}}(3) = \frac{1}{10}[-2\hat{x}(0) + \hat{x}(1) + 4\hat{x}(2) + 7\hat{x}(3)]
\tag{B-38}
$$

Therefore, we have obtained the causal FIR filter structure

$$
\hat{\hat{x}}(3) = \frac{7}{10}\hat{x}(3) + \frac{4}{10}\hat{x}(2) + \frac{1}{10}\hat{x}(1) - \frac{2}{10}\hat{x}(0)
\tag{B-39}
$$

or,

$$
\hat{\hat{x}}(k) = 0.7\hat{x}(k) + 0.4\hat{x}(k-1) + 0.1\hat{x}(k-2) - 0.2\hat{x}(k-3)
\tag{B-40}
$$

This is a weighted sum of the current and previous state estimates. Note that the current state estimates ($\hat{x}(k)$) are weighted the heaviest as expected. The deleterious effects of measurement noise on $\hat{\hat{x}}(3)$ have now been removed. In addition, an estimate of the vehicle's velocity is obtained.

Therefore, kinematic GPS addresses and mitigates the ill effects of measurement noise. We'd like to think of the proposed method as 'Indirect Kinematic GPS' or IKGPS. The algorithm is based on batch processing of the data. The data consists of a moving window. The ensuing algorithm is an FIR filter, albeit not all its' weights are positive, although the sum of the weights is always equal to 1, i.e.

$$
\sum weights = 1
\tag{B-41}
$$

A proposition is that the sum of the weights of the FIR filter for position estimation is always equal to 1. In addition, the sum of the weights of the FIR filter for velocity estimation is always equal to zero.

Bibliography

[1] Tobe' Corazzini and Jonathan How, "Onboard GPS Signal Augmentation For Formation Flying", Stanford University, 1998

[2] Tobe' Corazzini, Andrew Robertson, John Carl Adams, Arash Hassibi, and Jonathan P. How, "GPS Sensing for Spacecraft Formation Flying", Stanford University, 1997

[3] Duncan B. Cox and John D. W. Brading, "Integration of LAMDA Ambiguity Resolution with Kalman Filter for Relative Navigation of Spacecraft", ION 55th Annual Meeting, June 1999

[4] Jonathan P. How, Robert Twiggs, David Weidow, Kathy Hartman, and Frank Bauer, "Orion: A Low-Cost Demonstration of Formation Flying In Space Using GPS", *American Institute of Aeronautics and Astronautics, 1998*

[5] http://spacetechnology3.jpl.nasa.gov/proj/index.html

[6] Kaplan, Elliott D. *Understanding GPS, Principles and Applications*. Boston: Artech House, Inc., 1996.

[7] Zuofa Li, and Yang Gao, "Construction of High Dimensional Ambiguity Transformations for the LAMDA Method", University of Calgary, 1999

[8] Eric A. Olsen, Chan-Woo Park, and Jonathan How, "3D Formation Flight using Differential Carrier-phase GPS Sensors", Stanford University, 1998

[9] J. F. Raquet, Captain, USAF, Class Notes, 1999

[10] P. J. G. Teunissen, P. J. De Jonge, and C. C. J. M. Tiberius, "Performance of the LAMDA Method for Fast GPS Ambiguity Resolution", *Journal of The Institute of Navigation*, Vol. 44, No. 3, Fall 1997

[11] Sien-Chong Wu and Thomas Yunck, "Precise Kinematic Positioning with Simultaneous GPS and Carrier Phase Measurements", Jet Propulsion Laboratory, California Institute of Technology

[12] Brian J. Young, *An Integrated Synthetic Aperture Radar/GPS/INS System For Target Geolocation Improvement*, AFIT, 1999

1. AGENCY USE ONLY (Leave blank)	2. REPORT DATE	3. REPORT TYPE AND DATES COVERED
	March 2000	Master's Thesis

4. TITLE AND SUBTITLE
STOCHASTIC MODELING-BASED DGPS ESTIMATION ALGORITHM

5. FUNDING NUMBERS

6. AUTHOR(S)
James T. Broaddus, 1Lt, USAF

7. PERFORMING ORGANIZATION NAME(S) AND ADDRESS(ES)
Air Force Institute of Technology
2950 P Street
Wright-Patterson AFB, OH 45433

8. PERFORMING ORGANIZATION REPORT NUMBER

AFIT/GE/ENG/00M-06

9. SPONSORING/MONITORING AGENCY NAME(S) AND ADDRESS(ES)
Andy Proud, Capt, USAF
AFRL/SNAR
Wright-Patterson AFB, OH 45433
(937)255-5668

10. SPONSORING/MONITORING AGENCY REPORT NUMBER

11. SUPPLEMENTARY NOTES
Dr.Meir Pachter, Thesis Advisor
(937) 255-3636
meir.pachter@afit.af.mil

12a. DISTRIBUTION AVAILABILITY STATEMENT
Approved For Public Release; Distribution Unlimited

12b. DISTRIBUTION CODE

A

13. ABSTRACT (Maximum 200 words)

A Kinematic Differential Global Positioning System (KDGPS) algorithm is developed. A number of mobile receivers is considered, on of which will be designated the 'reference station' which will have known position and velocity information at the beginning of the time interval examined. Satellite clock biases are used to model Selective Availability. The measurement situation on hand is properly modeled and a centralized estimation algorithm processing several epochs of data. The effect of uncertainty in the reference receiver's position and the level of receiver noise is examined. Monte Carlo simulations are performed to examine the ability of the algorithm to correctly estimate the non-reference mobile user's position and velocity despite substantial satellite clock errors and receiver measurement noise.

14. SUBJECT TERMS
GPS, Global Positioning System, Differential, Satellite

15. NUMBER OF PAGES
83

16. PRICE CODE

17. SECURITY CLASSIFICATION OF REPORT	18. SECURITY CLASSIFICATION OF THIS PAGE	19. SECURITY CLASSIFICATION OF ABSTRACT	20. LIMITATION OF ABSTRACT
Unclassified	Unclassified	Unclassified	UL

GENERAL INSTRUCTIONS FOR COMPLETING SF 298

The Report Documentation Page (RDP) is used in announcing and cataloging reports. It is important that this information be consistent with the rest of the report, particularly the cover and title page. Instructions for filling in each block of the form follow. It is important to *stay within the lines* to meet *optical scanning requirements.*

Block 1. Agency Use Only *(Leave blank).*

Block 2. Report Date. Full publication date including day, month, and year, if available (e.g. 1 Jan 88). Must cite at least the year.

Block 3. Type of Report and Dates Covered. State whether report is interim, final, etc. If applicable, enter inclusive report dates (e.g. 10 Jun 87 - 30 Jun 88).

Block 4. Title and Subtitle. A title is taken from the part of the report that provides the most meaningful and complete information. When a report is prepared in more than one volume, repeat the primary title, add volume number, and include subtitle for the specific volume. On classified documents enter the title classification in parentheses.

Block 5. Funding Numbers. To include contract and grant numbers; may include program element number(s), project number(s), task number(s), and work unit number(s). Use the following labels:

C - Contract	PR - Project
G - Grant	TA - Task
PE - Program	WU - Work Unit
Element	Accession No.

Block 6. Author(s). Name(s) of person(s) responsible for writing the report, performing the research, or credited with the content of the report. If editor or compiler, this should follow the name(s).

Block 7. Performing Organization Name(s) and Address(es). Self-explanatory.

Block 8. Performing Organization Report Number. Enter the unique alphanumeric report number(s) assigned by the organization performing the report.

Block 9. Sponsoring/Monitoring Agency Name(s) and Address(es). Self-explanatory.

Block 10. Sponsoring/Monitoring Agency Report Number. *(If known)*

Block 11. Supplementary Notes. Enter information not included elsewhere such as: Prepared in cooperation with....; Trans. of....; To be published in.... When a report is revised, include a statement whether the new report supersedes or supplements the older report.

Block 12a. Distribution/Availability Statement. Denotes public availability or limitations. Cite any availability to the public. Enter additional limitations or special markings in all capitals (e.g. NOFORN, REL, ITAR).

DOD	-	See DoDD 5230.24, "Distribution Statements on Technical Documents."
DOE	-	See authorities.
NASA	-	See Handbook NHB 2200.2.
NTIS	-	Leave blank.

Block 12b. Distribution Code.

DOD	-	Leave blank.
DOE	-	Enter DOE distribution categories from the Standard Distribution for Unclassified Scientific and Technical Reports.
NASA	-	Leave blank.
NTIS	-	Leave blank.

Block 13. Abstract. Include a brief *(Maximum 200 words)* factual summary of the most significant information contained in the report.

Block 14. Subject Terms. Keywords or phrases identifying major subjects in the report.

Block 15. Number of Pages. Enter the total number of pages.

Block 16. Price Code. Enter appropriate price code *(NTIS only).*

Blocks 17. - 19. Security Classifications. Self-explanatory. Enter U.S. Security Classification in accordance with U.S. Security Regulations (i.e., UNCLASSIFIED). If form contains classified information, stamp classification on the top and bottom of the page.

Block 20. Limitation of Abstract. This block must be completed to assign a limitation to the abstract. Enter either UL (unlimited) or SAR (same as report). An entry in this block is necessary if the abstract is to be limited. If blank, the abstract is assumed to be unlimited.